TÜBİTAK

TÜRKİYE BİLİMSEL VE
TEKNİK ARAŞTIRMA KURUMU

THE SCIENTIFIC AND TECHNICAL
RESEARCH COUNCIL OF TURKEY

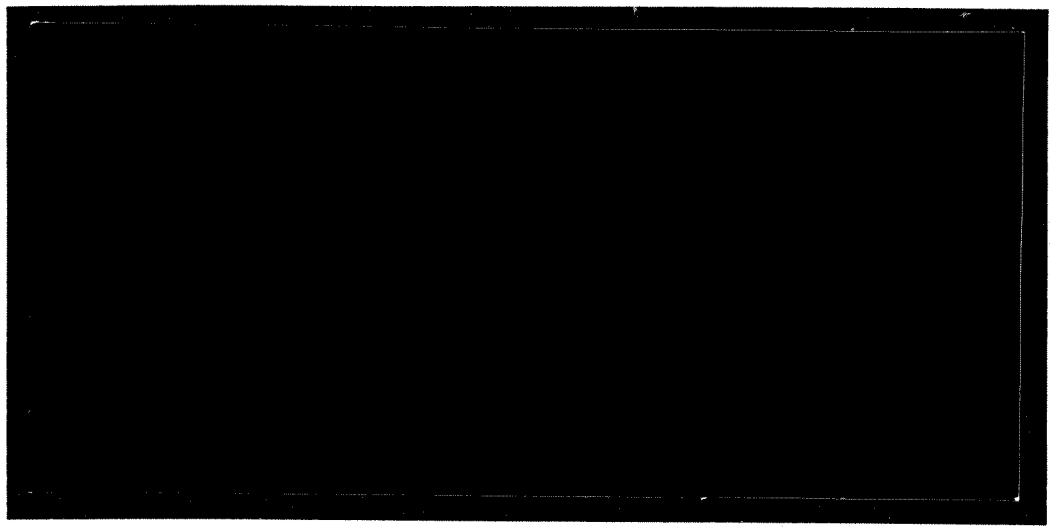

Temel Bilimler Araştırma Grubu

Basic Sciences Research Grant Committee

KLASİK-KUANTUM MOLEKÜLER DİNAMİK YÖNTEMİ İLE TİTREŞİM ENERJİSİ TRANSFERİ

PROJE NO: TBAG-1218

Prof.Dr.Ersin Yurtsever, Hülya Günay, Pasl A. Jalel

Orta Doğu Teknik Üniversitesi
Kimya Bölümü

Nisan 1995

ÖNSÖZ

Bu projede titreşim enerjisi transferi problemi, hem klasik mekanik yöntemlerle ve hem de kuantum etkilerin katıldığı Mixed-mode (MM) yöntemi ile incelenmektedir. Bu amaçla gerekli bilgisayar yazılımları geliştirilmiş ve uygulanmıştır. Bu proje TÜBİTAK Temel Bilimler Araştırma Grubu tarafından (TBAG-1218) desteklenmiştir.

İÇİNDEKİLER

ÖZ

Moleküliçi titreşim enerjisinin transferi, kontrollü reaksiyonları gerçekleştirmek isteyen bilim adamları için çok önemli bir konudur. Bu olayların mekanizmaları ve zaman ölçekleri, molekülde seçilmiş bağların oluşması veya kırılması için gerekli bilgiyi sağlarlar. Dinamik bir problemin kuantum mekaniksel analizi hesap zamanı açısından büyük güçlükler gösterir, buna karşılık klasik mekanik yöntemler ise sıfır noktası enerjisi veya tünelleme gibi olayları içermemeleri nedeni ile hatalı sonuçlara neden olabilirler. Bu çalışmada, her iki yaklaşımı birleştiren bir yöntem sunulmuş ve değişik uygulamaları tartışılmıştır. SCF yaklaşımı içerisinde problemin bir kısmı kuantum mekaniksel yollarla çözülmüş ve diğer kısımları ise klasik mekanik kanunlarınca yorumlanmıştır. Özellikle klasik kaosun, kısmi kuantumlaşma altında gösterdiği değişiklikler, kuantum dalgapaketine karşılık olabilecek faz uzayının tanımı ve bir boyutlu zincir üzerinde enerjinin transferi soruları çalışılmış, değişik çözüm yöntemleri geliştirilmiş ve bazı ipuçları elde edilmiştir.

Anahtar kelimeler/ kuantum dinamiği, kaos, enerji transferi

ABSTRACT

Vibrational energy transfer in molecules is an important problem for the ultimate aim of controlled reactions. The mechanisms and time scales of these processes give us the information necessary to form or break preselected bonds in a molecule. Quantum mechanical analysis of a dynamical problem is computationally prohibitive whereas the classical mechanics suffer from the inability to incorporate effects such as zero-point energy or tunneling. In this work a method which compromises both approaches has been presented and it various applications are discussed. Within the SCF approximation, part of the problem is solved under quantum mechanical considerations and the other parts are treated classically. The specific questions of what happens to the classical chaos under partial quantization, what is the corresponding phase space description of a quantum wavepacket and how the energy is transferred along a one-dimensional chain are studied, various solution methods are developed and certain clues are obtained.

keywords/ quantum dynamics, chaos, energy transfer

GİRİŞ

Moleküliçi enerji transferinde rol oynayan faktörlerin bulunmasında, ele alınan problemin büyüklüğüne ve karmaşıklığına göre değişik yöntemler kullanılmaktadır. Problemin doğru olarak anlaşılması zamana bağlı Scrödinger denkleminin çözümü ile mümkünse de, çok küçük sistemler (3-4 boyutlu problemler) dışında saysısal açıdan pratik sonuçlar alınamamaktadır. Teorik olarak yöntemler uzun zamandan beri bilinmekte ise de, günümüzün süperbilgisayarlarında bile nispeten büyük bir molekülün kuantum dinamiğini incelemek mümkün olmamaktadır. Bu durumlarda klasik mekaniğin herhangibir formalizmini kullanarak dinamik özelliklerin hesabı (bizim durumumuzda titreşim enerjisinin moleküliçinde transferi) yapmak zorunda kalınmaktadır. İster Newton veya Lagrange ister Hamilton denklemleri kullanılsın, çok yüksek boyutta problemlerin (eğer kısa mesafeli potensiyel fonksiyonları kullanılıyorsa milyonlarca parçacığın simülasyonu pek zor değildir) çözümleri bulunmakta fakat klasik mekaniğin temelinde yatan eksiklikler ciddi hatalara yol açmaktadır. En basit yaklaşımla, tünelleme veya sıfır-noktası enerjisi gibi kavramların klasik mekanikte yerinin olmaması, enerji transferinde önemli bazı sorunları da beraberinde getirmektedir. Hem kuantum mekaniğinin öngördüğü koşulların sağlanması ve hem de klasik mekanik yöntemlerin sayısal kolaylıklarından yararlanmak için bazı hibrid yöntemlerin denenmesi gerekmektedir. Bunlardan Carr-Parinello adı verilen yaklaşımda klasik dinamik denklemler, her adımda yaklaşık kuantum yöntemlerle hesaplanan potensiyeller altında çözülmektedir. Uzun vadede çok yararlı olabilecek bu yaklaşım, halen gereksinme duyulan bilgisayar zamanlarının çokluğu nedeni ile yeteri derecede kapsamlı olarak uygulanamamaktadır.

Başka bir alternatif yaklaşım ise sistemdeki titreşim modlarının özelliklerinin farklılığından yararlanarak, bir klasik-kuantum karmaşık yöntemin (Mixed-mode MM) geliştirmeye yönelikdir. Moleküllerin elektronik yapısının belirlenmesinde kullanılan ilk yaklaştırma Born-Oppenheimer yaklaştırması olup, atom çekirdeklerinin elektronlara göre çok daha ağır olmaları nedeni ile daha yavaş hareket edecekleri ve böylelikle dalga fonksiyonunun çekirdek ve elektronik dalga fonksiyonunun çarpımı olarak yapılabileceği esasına dayanır. Böylelikle her nükleer geometride yapılacak olan kapsamlı bir elektronik hesap ile, molekül içi hareket iki kısma ayrılacak ve elektronlar kuantum yöntemlerle çalışılırken, çekirdeklerin hareketi bir klasik felsefede incelenecektir. Gerektiği takdirde bu iki hareketin birleştirilmesi bazı yaklaşık ifadelerle sonradan yapılabilir. Buna benzer bir yaklaşımı titreşim hareketine taşımak mümkündür. Titreşim modlarını frekanslarına veya incelenen probleme yapmakta olduğu katkılara göre sınıflandırabiliriz. Örneğin çok hızlı hareket eden (sert) modları kuantum yöntemlerle ama daha yavaş olan yumuşak modları da klasik mekaniksel yöntemlerle çözebiliriz. Başka bir yönden ise, modları işlevlerine göre ayırabiliriz, örneğin bir Langevin tipi adsorpsiyon modellemesinde, yüzeydeki ilk parçacıkla adsorbant arsındaki etki kuantize olmak zorunda olduğu halde, yüzeyin diğer parçacıklarının birbirleriyle etkileşmesi klasik olarak incelenebilir. Bu ayrımlar yapıldığı takdirde, küçük boyutlarda kuantum problemleri büyük çapta klasik alanların etkisi altında çözülebilecektir.

Bu proje çerçevesinde böyle bir yöntemin esasları belirlenmiş, bazı sorulara yanıtlar bulunmuş ve değişik problemlere uygulamalarının bir kısmı bitmiş ve bir kısmında da çalışmalar devam etmektedir. Yapılan işler şu başlıklar altında toplanabilir.

a) Self-consistent-field (SCF) yaklaşımı altında klasik ve kuantum dinamik denklemlerinin beraber çözümü için yöntemler
b) Klasik anlamda kaos gösteren titreşim hareketlerinin, kısmi kuantumlaşma altındaki davranışları
c) Klasik, kuantum veya MM sonuçlarının karşılaştırılabilmesi açısından, belirli bir dalga paketine karşılık gelen klasik parçacıkların seçimi
d) Zaman bağlı Schrödinger denkleminin, Hamilton formalizmine benzer bir şekilde çözümü
ve
e) Zincir üzerinde enerji transferi olayının modellenmesi ve MM çözümleri.

SCF YAKLAŞIMI

Klasik ve kuantum denklemlerinin aynı anda çözümleri mümkün olmadığı için, elektronik hesaplarda kullanılan kendiyle çelişmeyen özuyumlu alan (self-consistent-field SCF) denklemlerinin bu sahaya bir uyarlaması gerekmektedir. Örnek olarak iki boyutlu bir problemi aldığımız zaman, bunu iki ayrı ama birbirinin etkisi altında hareket eden denklem halinde yazabiliriz. Bu doğal olarak çözüme bir hata getirmektedir, bununla beraber biraz önce değinildiği gibi hem Schrödinger denklemini ve hem de Hamilton denklemlerini tek bir denklem setine dönüştürmek de olası değildir. İki boyutta bir Hamiltonyeni yazarsak (daha fazla boyutlara taşımak basittir):

$$H = H_x + H_y + V(x,y)$$

eğer V(x,y) ayrıştırılamayan bir bağlantı terimi ise, SCF yaklaştırması altında şu hale getirilebilir:

$$H_x^{SCF} = H_x + \langle V \rangle_y \quad \text{ve} \quad H_y^{SCF} = H_y + \langle V \rangle_x$$

Burada $\langle V \rangle_x$, x koordinatı üzerinden ortalama alınmış bir ifadeyi belirler. Şimdi bu iki ayrı hareket denkleminin çözümleri yapılabilir. İteratif olarak başlangıç koşulları belirlendikten sonra, örnek olarak x koordinatındaki denklem, y üzerinden ortalama alınmış olan potensiyelin etkisi altında çözülür ve aynı işlem de y boyutunda tekrarlanır. Herzaman adımında x ve y koordinatlarındaki değişkenler (konumlar, momentumlar veya dalga fonksiyonları) değişeceği için etki eden potensiyel fonksiyonları da kapalı bir şekilde zamana bağımlılık göstereceklerdir. Eğer zaman adımı yeteri derecede küçük ise, sabit potensiyel kullanımından (zaman adımı süresince) gelen hata da küçük olacaktır. Bizim MM yaklaşımımızda ise denklemlerin biri klasik ve diğeri de kuantum karakterinde olacağı için şöyle yazılacaktır.

$$\partial p_x / \partial t = - \partial H_x^{SCF} / \partial x$$

$$\partial x / \partial t = \partial H_x^{SCF} / \partial p_x$$

ve

$$i\hbar \partial \psi (y,t) / \partial t = H_y^{SCF} \psi (y,t)$$

Başlangıç koşulları ise x boyutunda bir parçacık (koordinat ve momentumu ile belirlenmiş) ve y boyutunda bir dalga paketi ile tanımlanır. Genelde dalga paketi ya bir minimum belirsizlik dalga paketi veya özfonksiyonların bir bileşimi olarak yazılır. Her iki halde de harmonik (veya anharmonik) özfonksiyonlar cinsinden açılımı yazmak hesaplar açısından kolaylık getirmektedir. Başlangıç koşulları belirlendikten sonra iki boyut üzerinden ortalamalar alınır. Klasik parçacık üzerinden ortalama ancak birden fazla trajektoriden oluşan bir paket varsa yapılır, aksi takdirde tek bir değer kullanılır; dalga paketi üzerinden ise bir beklenen değer integrali hesaplanır. Kısa bir zaman adımı için yukarıda verilen denklemlere göre hem parçacığın yeni konumu ve hem de yeni dalga paketi bulunur. Bu işlemler yeterli veri toplanıncaya kadar devam edilir. Klasik denklemler sabit adımlı 4-adım Runge-Kutta sayısal integrasyonu ile çözülmüştür. Kuantum denklemlerin çözümü içen öngörülen bir yöntem, bu proje başlamadan önce yayınlanmıştı ve detaylı bilgi bu makalelerde verilmiştir (E.Yurtsever ve J.Brickmann, Berichte der Bunsenges.Phys.Chem. 96, 142-146 (1992) ile E.Yurtsever ve T.Uzer, ibid., 96, 902-913 (1992)). Daha sonra geliştirilen bir başka yöntem de biraz sonra anlatılacaktır. SCF yaklaşımının getirdiği hatalar ise 1994 yazında benim düzenlediğim bir yaz okulunda verdiğim ders içerisinde tartışılmıştır. Eğer klasik anlamda kaos gösteren bir sistem ile çalışılıyorsa, doğal olarak SCF ve tam çözümler birebir uyumlu olmayacaklardır. Kaotik denklemlerde yapılacak en küçük tedirginliklerin bile sistemi faz uzayında başka noktalar götürdükleri düşünülürse, bu normal karşılanmaktadır. Bununla beraber denklemlerin nitel davranışlarının değişmemesi gerekmektedir. Bunun anlamı, sisteme SCF yaklaştırması nedeni ile suni düzenliliklerin girmemesi şarttır, aksi takdirde klasik mekanik sonuçları ile karşılaştırılamaz. Şu ana kadar elde edilen sonuçlar bu açıdan tatminkar gözükmektedir ve Kluwer Press tarafından basılacak olan "Frontiers of Chemical Dynamics" kitabında yayınlanacaktır.

KISMİ KUANTUMLAŞMA

MM yaklaşımı ile bir sisteme etki eden dış etkenlerin klasik veya kuantum alanları olmalarının getireceği farklılıkları incelemek mümkündür. Gene iki boyutlu problemi ele alıp, bunlardan bir boyutunu klasik parçacık olarak tanımlayalım. Diğer boyutu ise bir hesap grubunda klasik parçacık olarak diğerinde ise bir kuantum dalga paketi olarak seçelim. Klasik ve kuantum dinamiğinin karşılaştırılmasındaki en büyük sorun, farklı karakterdeki ölçümlerin nasıl karşılaştırılacağıdır. Dalga paketi üzerinden alınan ortalama değerlerle, klasik parçacığın özelliklerini göreceli olarak anlamanın kolay bilinen bir yöntemi yoktur. Ama MM yaklaşımında, bir boyut hep klasik kalacağı

için, o boyuta ait ölçümleri klasik ve kuantum alanlar altında yapıp karşılaştırabiliriz. Bu çalışmada klasik parçacığın koordinatının, momentumunun, enerjisinin ve bağlantı terimindeki enerjinin zamana göre değişimleri hem 2-boyutlu klasik sistem için ve hem de MM sistemi için yapılmıştır. Elde edilen zaman serilerinin periyodiklik testleri gerek otokorelasyon fonksiyonları ve gerekse de Fourier analizleri ile yapılmıştır. Sonuçta benzer şartlar altında gerçekleştirilen sistemlerden, kısmi kuantumlaştırılmış olanlarında çok daha fazla düzenlilik görülmüştür. Bu bulgular Phys.Rev.E, 50, 3422-3430 (1994) de yayınlanmıştır.

DALGA PAKETİ-PARÇACIK BENZERLİĞİ

Klasik ve kuantum mekaniğinin sonuçlarının karşılaştırılmasındaki en önemli güçlük, birbirine karşılık gelen gösterimlerin bulunmasıdır. Kuantum mekaniğindeki başlangıç koşulu bir dalga paketi olsun. Schrödinger denkleminin çözümü ile elde edilen dinamik özellikleri, klasik bir parçacığın hareketi ile karşılaştırmak istediğimizde beliren sorun, klasik parçacığın başlangıç koşulları olarak hangi koordinat ve momentum değerlerini alacağımızdır. Daha doğrusu dalga paketi bir dağılım fonksiyonu olduğu için, aslında bir değil çok sayıda başlangıç koşulunun bu dalga paketine karşılık olması gerekir. Aynı soruyu diğer yönden de sorabiliriz. Eldeki bir dizi klasik parçacığa karşılık gelen dalga paketi nedir? Bu sorunun tam bir cevabı yoktur. Yukarıda anlatılan problem için, enerjilerin ve koordinat ile koordinat beklenen değerlerinin aynı olduğu koşullar seçilmişti. Dalga paketinin klasik karşıtı için önerilen ilk yöntem Wigner dönüştürmesidir.

$$W(q,p) = \frac{1}{2\pi\hbar}\int_{-\infty}^{\infty} \psi^*\left(q+\frac{x}{2}\right)\psi\left(q-\frac{x}{2}\right)e^{\frac{ixp}{\hbar}}dx$$

Bu integral bir probabilite dağılımı olarak sadece asimptotik değerlerde doğrudur. Doğal olarak klasik faz uzayının bazı bölgelerinde negatif olacağı için, bir probabilite dağılımı olarak kullanılması zordur. Wigner dağılımının, bir Gaussian ile düzgünleştirilmiş hali ise Husimi dönüştürmesi olarak adlandırılır ve hernekadar matematiksel bir ispatı yok ise de her yerde pozitif olması nedeni ile probabilite dağılımı olarak kullanılabilir.

$$\rho_H(q,p) = \left[\int_{-\infty}^{\infty} \exp\left[-\frac{1}{\omega^2}(x-q)^2 + ipx\right]\psi(x)\,dx\right]^2$$

Bu konudaki çalışmamızda, bir dalga paketinin Husimi dönüştürmesini ağırlık fonksiyonu alarak 1000-2000 civarında klasik başlangıç koşulu seçtik. Burada Monte Carlo tipi bir yaklaşım kullandık. Önce bir örgü üzerindeki her noktada dalga fonksiyonunun Husimi dönüşümünü hesapladık. Dalga paketi harmonik sarkaç özfonksiyonları cinsinden yazıldığı için bu integraller analitik olarak bulunabilir. Daha

sonra verilen enerji bölgesi içerisinde seçilen rastgele noktalardaki Husimi dağılımının değeri gene yeni seçilmiş bir rastgele sayı ile karşılatırıldı. Böylelikle Husimi ağırlıklı noktalardan oluşan bir klasik parçacık demeti elde edildi. Bu demetteki parçacıkların enerjileri sabit değil ama bir enerji bantı üzerine düşmekteydi. Bu başlangıç koşulundan yapılan simülasyonlar ile dalga paketinin zaman içerisindeki değişimini karşılaştırdığımızda bazı benzerlikler gördük. Böylelikle elde edilen noktalarla yaptığımız iki boyutlu sistemlerin Lyapunov üstellerinde ise çok belirgin olmayan bazı farklılıklara da rastlandı. Bulunan grafiksel bulgular Tr.J.Physics, 18 1095-1105 (1994) de yayınlandı. Bu problemin daha detaylı çalışmalarının yapılması planlanmaktadır.

HAMILTON TİPİ KUANTUM DİNAMİĞİ

Kuantum dinamiğinin temel denklemi olan Schrödinger denkleminin çözümü için değişik bir yöntem geliştirildi. Bu biraz sonra anlatılacak olan zincir üzerinde enerji transferi problemi için de oldukça büyük bir kolaylık getirmekte. Anlatılacak olan yöntem, formalizm olarak daha önce de önerilmiş olmakla beraber kapsamlı uygulamasına rastlanamamıştır. Bunun da nedeni MM'a geçmekte çok yararlı olması ama normal bir kuantum dinamiği için belki de grid yöntemlerinden çok daha kolay olmaması düşünülebilir.

Bir dalga paketini herzaman Hermityen bir operatörün özfonksiyonlarının cinsinden yazabiliriz.

$$\psi (q,t) = \Sigma c_k(t) \varphi_k (q)$$

Zaman bağlı doğrusal katsayılar ise kompleks oldukları için, gerçek ve sanal bileşenlerine ayrılırlar.

$$c_k = x_k + i p_k$$

Şimdi Schrödinger denklemini atomik birimlerde yazarsak:

$$i \Sigma \varphi_k (x_k + i p_k) = \Sigma (x_k + i p_k) H \varphi_k$$

Soldan φ_m ile çarpıp integralini aldığımız zaman , dalga fonksiyonlarının ortogonalliği nedeni ile, denklem şu hale dönüşür.

$$i (x_m + i p_m) = \Sigma (x_k + i p_k) H_{mk}$$

H_{mk} Hamiltonyenin bir matris elemanıdır ve kompleks de olacağı gözönüne alınırsa :

$$H_{mk} = a_{mk} + i b_{mk}$$

olarak yazılabilir ve denklemin her iki tarafının gerçek ve sanal kısımların ayrı ayrı eşitlersek şu iki denklem ortaya çıkar:

$$x_m = \Sigma\, x_k\, b_{mk} + p_k\, a_{mk}$$

ve

$$p_m = \Sigma\, -x_k\, a_{mk} + p_k\, b_{mk}$$

Eğer yeni bir Hamiltonyen ifadesini tanımlarsak:

$$\mathbf{H} = 0.5\, \Sigma\Sigma\, (x_m - i\, p_m)\, (x_k + i\, p_k)\, H_{mk}$$

Bu ifadenin x_k ve p_k'ya göre türevlerini, bir önceki denklemlerde verilen zamana göre türevler cinsinden yazarsak:

$$\partial\, p_m / \partial\, t = - \partial\, \mathbf{H} / \partial x_m$$

$$\partial\, x_m / \partial\, t = \partial\, \mathbf{H} / \partial\, p_m$$

Bu denklemler de bildiğimiz klasik mekaniğin Hamilton denklemleridir ve çözümleri için pekçok yöntem uygulanabilir. Buna ek olarak bu denklemleri Newton formalizminde yazmak ve dolayısı ile Gear, Verlet gibi sistemlerin simplektik yapısını koruyan hızlı yöntemleri uygulamak mümkündür. Son elde edilen denklemlerle kuantum dinamiğinin bir ve iki boyutlu problemlere uygulanması da Ber.Bunsenges.Phys.Chem. 98, 554-559 (1994) ve ibid, 98, 1552-1562 (1994) de yayınlanmıştır.

ZİNCİR ÜZERİNDE ENERJİ TRANSFERİ

İki boyuttan daha büyük sistemlere örnek olarak tek boyutlu zincir üzerinde enerjinin transferi seçilmiştir. Burada model olarak birbirine nonlineer bağlı, parçalanmayan sarkaçlar seçildi. Ara raporlarda bu problemin formülasyonunda beliren sorunlar anlatılmıştı. Böyle bir sistemi parçacıkların, bağların veya normal modların etkileşmesi olarak yazmak mümkündür. Herbir yaklaşım klasik mekanik yöntemlerde aynı kolaylıkta ise de MM yaklaşımında ortaya çıkan sorunlardır. O rapordan bu yana geçen süre zarfında bu sorunlar halledilmiş olup, veriler sürekli olarak yaratılmaktadır. Parçacık bazında ele alındığında Hamiltonyen şu şekilde yazılmaktadır:

$$H = 0.5\, \Sigma\, p_k^2/m_k + \Sigma\, a_k\, (x_{k+1}-x_k)^2 + \Sigma\, b_k\, (x_{k+1}-x_k)^3 + \Sigma\, c_k\, (x_{k+1}-x_k)^4 + \Sigma\, d_k\, (x_{k+1}-x_k)^2 (x_{k+2}-x_{k+1})^2$$

Bu gösterim MM felsefesinde kavramsal güçlükler çıkarmaktadır. Kuantize olması gereken birimin parçacık değil etkileşme olması gerekir. Parçacık gösteriminde ise

kinetik enerji terimlerini ayrıştırmak (MM yaklaşımında) ve bağların kinetik enerjilerini bulmak oldukça zordur. Eğer bağ gösterimine aşağıdaki şekilde geçersek:

$q_k = x_{k+1} - x_k$

Hamiltonyen ifadesi şu şekli alır:

$$H = 0.5 \Sigma p_k^2/\mu_k + \Sigma a_k q_k^2 + \Sigma b_k q_k^3 + \Sigma c_k q_k^4 + \Sigma d_k q_{k+1}^2 q_k^2 - \Sigma p_k p_{k+1}/m_{k+1}$$

Tabii bu gösterimden normal modlara da geçmek söz konusu olabilir fakat anharmonik terimlerin bulunması nedeni ile çok yararlı olmamaktadır. Bu gösterimin sorunu da en sonda verilen momentum bağlantı terimlerindedir. Momentum operatörünün kompleks olması, kuantum Hamiltonyeninin gerçek olma özelliğini bozmakta ve problemi sıradan bir özdeğer probleminden, kompleks özdeğer problemine dönüştürmektedir. Bu da milyonlarca defa yapılacağı düşünülen bir hesap için ciddi sorunlar oluşturmaktadır. Bununla beraber bir önceki kısımda anlatıldığı gibi Hamilton denklemlerine benzer çözüm yöntemleri bu sorunu ortadan kaldırmaktadır. SCF yaklaşımında kuantum denklemi şu halde yazılır:

$$H^0 = -0.5/\mu_n \, d^2/dq^2 + a_n q_n^2 + b_n q_n^3 + c_n q_n^4 + d_{n-1} q_{n-1}^2 q_n^2$$

$$H = H^0 - i\, 0.5\, p_{n-1}/ m_n \, d/dq_n$$

eğer dalgapaketi harmonik osilatör özfonksiyonları cinsinden yazılırsa:

$$\psi (q,t) = \Sigma c_k(t) \varphi_k (q)$$

Hamiltonyen matris elemanlarının ifadeleri açıkça aşağıdaki şekli alırlar:

$$H_{mk} = \delta_{mk} \varepsilon_m + b_n q^3_{mk} + c^n q^4_{mk} + d_{n-1} q_{n-1}^2 q^2_{mk}$$

$$- i\, 0.5\, p_{n-1}/ m_n \, D_{mk}$$

D ise türev operatörüdür. Bu şekilde gerçek ve sanal kısımları ayrılmış olan matris elemanları ile yukarıda verilen x_k ve p_k katsayılarının çözümleri bulunur.

Model olarak seçilen Hamiltonyende bütün osilatörler eşdeğer alınmıştır. Kullanılan parametreler m=1, a=0.5, b=0, ve c=0.25 olarak seçilmiştir. Başlangıç koşulları olarak da sonuncu hariç bütün osilatörler minimum enerji konumuna yerleştirilmişlerdir (q=0 ve p=0). Bir uçtaki sarkaç ise belirli uzaklıklara çekilmiş (minimum enerji konumundan uzaklaştırılmış) ve sıfır momentum verilmiş olarak yerleştirilmiştir. Böylelikle gerilmiş bir zincirin gevşemesi modellenmiş olacaktır. İlk olarak klasik mekanik simülasyonlar değişik gerginlikler (dolayısı ile değişik enerjiler) ve d_{n-1} bağlanma katsayıları için yapılmıştır. Sistemin dinamiğinin kaotik veya düzenli oluşunu tanımlayan ölçek olarak genelde en büyük Lyapunov üsteli kullanılır. Bu üsteller faz uzayında birbirine çok yakın konumda başlayan hareketlerin zaman içerisinde ne kadar birbirlerinden uzaklaştıklarını belirlerler. Eğer üstel 0 ise her iki hareketin de benzer kaldığı ve dolayısı ile dinamiğin düzenli

olduğu anlaşılır. Buna benzer olarak kullanılan bir başka ölçek de Kolmogorov entropisidir. Kullanılan zincir modelinde faz uzayı bağ sayısının iki katı (2N) boyutludur (tek boyut üzerinde olduğu için her bağı bir koordinat ve bir de momentum ile tanımlarız) ve sistemin de 2N Lyapunov üsteli vardır. Hamiltonyen sistemlerde faz uzayının hacmı sabit kalacağı için, Lyapunov üstellerinin de toplamı sıfır olmak zorundadır. Bu nedenle üstellerin bir kısmının sıfırdan büyük (eğer düzensiz bir dinamik var ise) ve diğerlerinin de sıfırdan küçük olması gerekir. Sıfırdan büyük olan üstellerin toplamına ise Kolmogorov entropi denir ve genelde nitel davranışları da maksimum Lyapunov üsteline paralel olur. Şekil 1 de Kolmogorov entropisinin, bağlantı parametresinin değerlerinin 0, 2, 4, ve 6 olduğu hallerde, son osilatörün boyu ile değişimini vermekteyiz. Toplam enerji ise bağlantı parametresi cinsinden E=0.5*X*X + 0.25*X*X*X*X olarak verildiği için, absisi enerji ekseni olarak da alabiliriz. Bu şeklin verdiği sonuç ise sistemin kaotik davranışında enerji akışını sağlayan bağlantı parametresinin bir etkisi olmadığı ve esas düzenlilik ile kaosun arasındaki geçişi belirleyen parametrenin toplam enerji olduğudur. Kolmogorov entropisinin birimi bit/zaman birimi olarak verilmiştir. Benzer olarak model zincirin boyunun uzatılmasının da dinamik karaktere etkisi gözlenmemiştir (daha uzun zincirler ile hesaplar yapılmış fakat farklı bir davranışa rastlanmamıştır).

Bu koşullarda, mixed-mode gösterimine geçildiği zaman, hesapların yoğun bilgisayar zamanına ihtiyaç göstermeleri nedeni ile bağlantı parametresi için d=1.0 alınmış ve uçtaki osilatörün uzunluğuna (dolayısı ile toplam enerjiye) göre enerji transferinin değişimi hem klasik ve hem de MM altında gözlenmiştir. MM hesaplarında başlangıç dalga paketi 20 harmonik osilatör özfonksiyonundan oluşan bir MUW (minimum uncertainty wavepacket) olarak alınmıştır.

$\Psi(MUW) = \Sigma\, c_k\, \varphi_k$

c_k ise $\exp(-0.5*a*a)\; a^k\; (k!)^{-1/2}$ olarak verilir. Buradaki a parametresi ise dalga paketinin yerleştirildiği klasik benzeri konum ve momentumdan oluşur.

$a = (0.5\, m\, w\, /\hbar)^{1/2}\; (x + i/(mw)\, p)$

Başlangıç koşullarının detaylı tanımları ise şöyledir. Klasik mekanik yöntemde bir önceki kısımda anlatılan koşullar alınmıştır. MM de ise, ilk (N-1) osilatör gene klasik olarak denge konumunda tanımlanmışlardır (x=0, p=0). Son osilatör ise kuantum dalga paketi olarak aynı enerjiyi verecek şekilde seçilmiştir. Her iki hesap da eş bir zaman sürecinde çözülmüş (MM hesaplarının kararlılığı için daha küçük zaman adımları kullanmak gerekmiştir) ve belirli aralıklarla hesaplanan pek çok özellik saklanmıştır.(Bu proje çerçevesinde alınan DAT sürücü ve disk son derece işe yaramıştır. genelde 4 osilatörlü bir sistemde yapılan tek bir hesap için 20 MB civarında disk alanına ihtiyaç belirmektedir; yoğun bilgisayar zamanı gerektiren hesapların sonuçlarının saklanması ise 800-900 Mblık bir alanı meşgul etmektedir).

Şekil 2 de ilk üç osilatörün ortalama enerjilerinin toplam enerji (başlangıç koşulu) ile değişimini hem klasik ve hem de MM yönteminde vermekteyiz. Kuantize edilen osilatörün 4 numaralı bağ olduğunu burada belirtelim. Genel eğilim, enerjinin uçtaki osilatöre kadar yayılabildiği fakat MM yaklaşımında bu yayılmanın klasik yöntemlere göre daha az miktarlarda olduğudur. Şekil 3 de ise bağların ulaştığı maksimum

boyutların değişimi verilmiştir ve sonuçlar, başlangıçta dengede olan bağların da büyük ölçüde enerji kazandığı, hareket ettiği fakat MM yaklaşımının bunu nispeten kısıtladığı yönündedir. Son olarak şekil 4 de 3 ve 4 numaralı bağların arasındaki kinetik ve potensiyel enerji bağlantı terimlerindeki ortalama enerjiler verilmiştir. Potensiyel enerji değerleri her iki yöntemde de farklılıklar göstermemekte ise de kinetik enerji eğrileri önceki grafiklere benzer özellikler vermektedir.

SONUÇ

Bütün bu verilerin sonucunda MM yaklaşımının enerji transferini yavaşlattığı ortaya çıkmaktadır. Bununla beraber bu yavaşlatmanın iki nedeni olabilir. Birincisi, sisteme katılan kuantum etkiler, diğeri ise SCF yaklaşımıdır. Bunların ayrı ayrı değerlendirilmeleri için gerekli teorik ve sayısal çalışmaların önumüzdeki bir-iki seneyi almaları söz konusudur. Buradaki önemli sorun klasik ve kuantum mekaniğini SCF yaklaşımı kullanmadan birlikte değerlendirebilecek bir yöntemin olmamasıdır. Klasik ve kuantum dinamiği, SCF'e benzer bir şekilde ayrı ayrı çözecek yöntemlerin incelenmesinde bazı ipuçlarının eldesi bu çalışmalara başlangıç olacaktır.

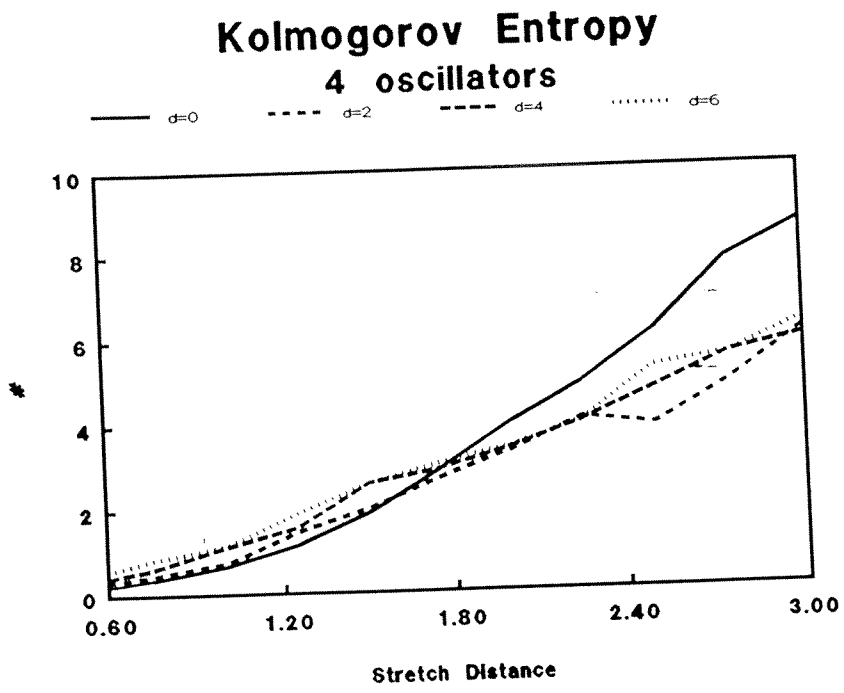

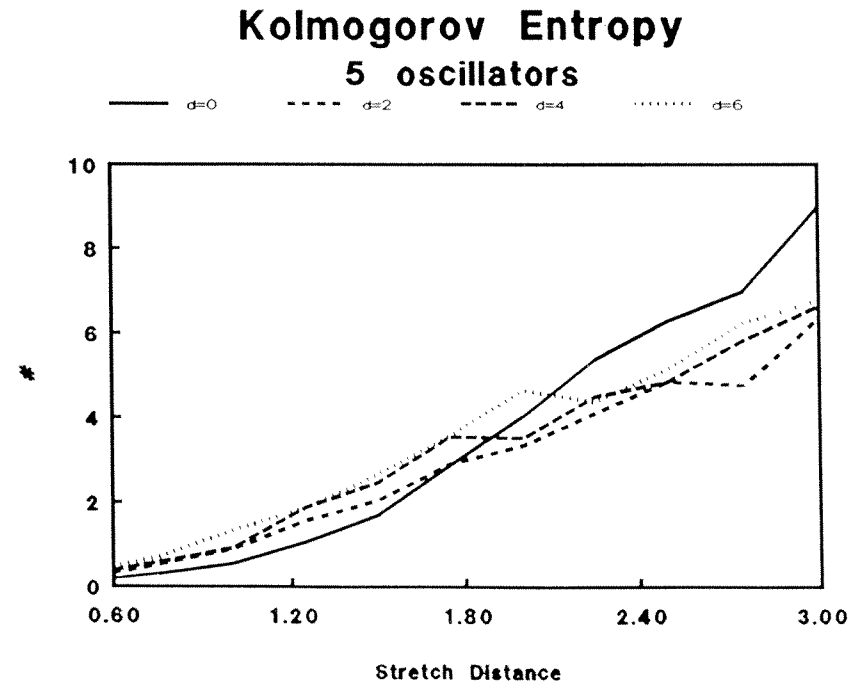

Şekil 1. Kolmogorov entropisinin 4 ve 5 osilatörden oluşan zincirlerde, uçdaki parçacığın konumuna (toplam enerjiye) göre değişimi. Eğriler farklı bağlanma parametrelerindeki sonuçları göstermektedir.

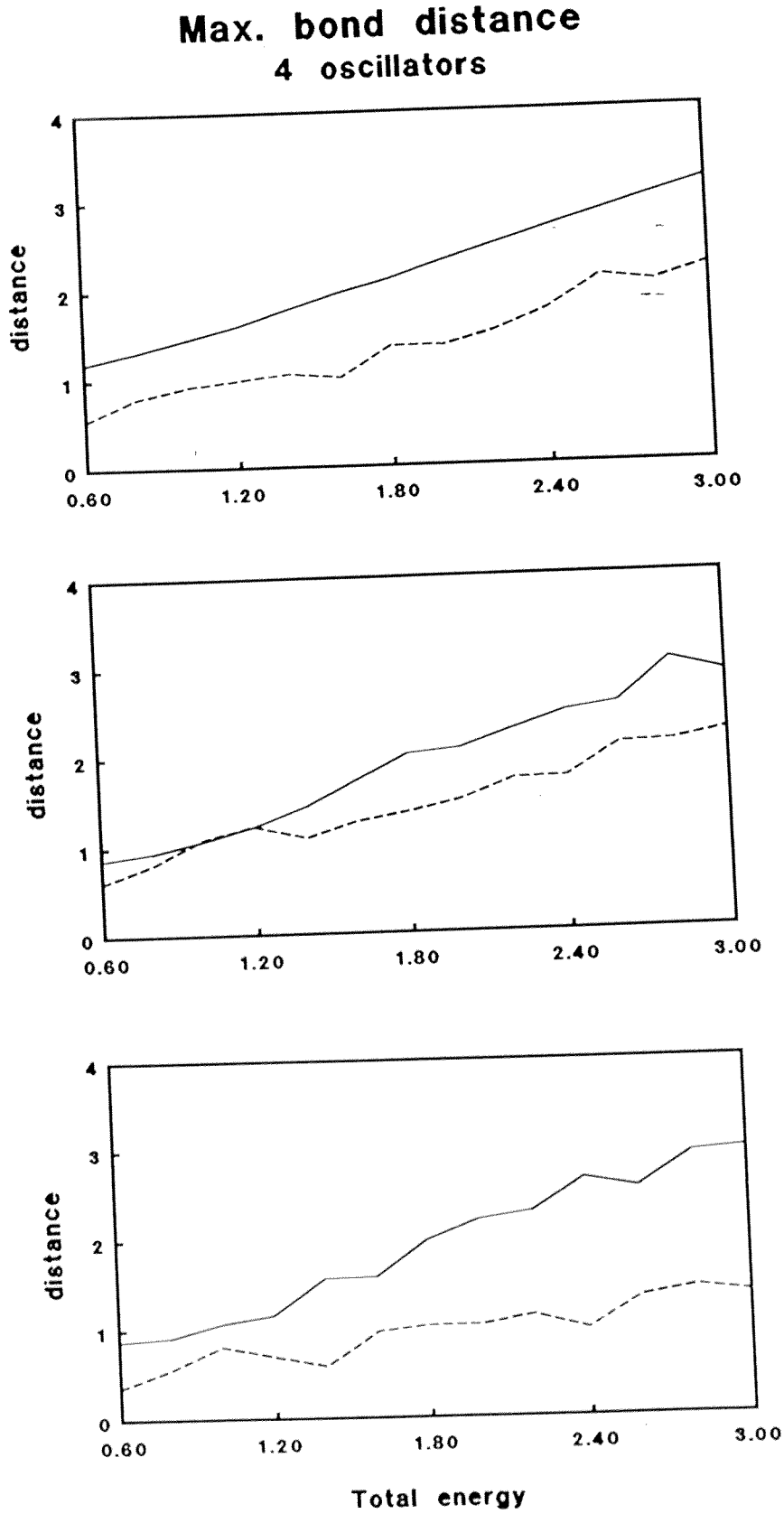

Şekil 3. Başlangıç değerleri denge konumları olan osilatörlerin ulaştığı maksimum gerilmelerin, toplam enerji ile değişimleri.
Klasik mekanik ———
Mixed-mode – – – –

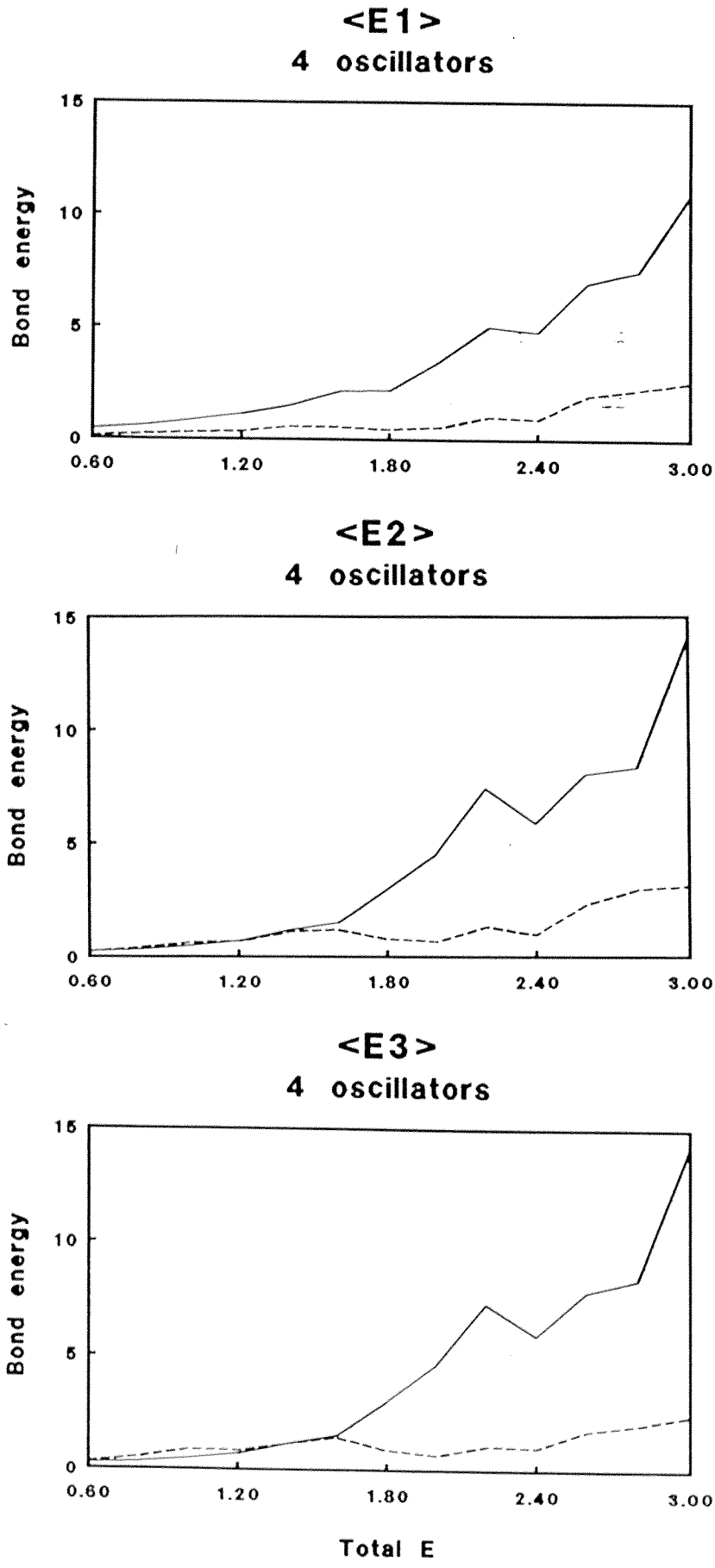

Şekil 2. Başlangıç değerleri denge konumları olan osilatörlerin ortalama enerjilerinin, toplam enerji ile değişimleri.
Klasik mekanik ——
Mixed-mode – – – –

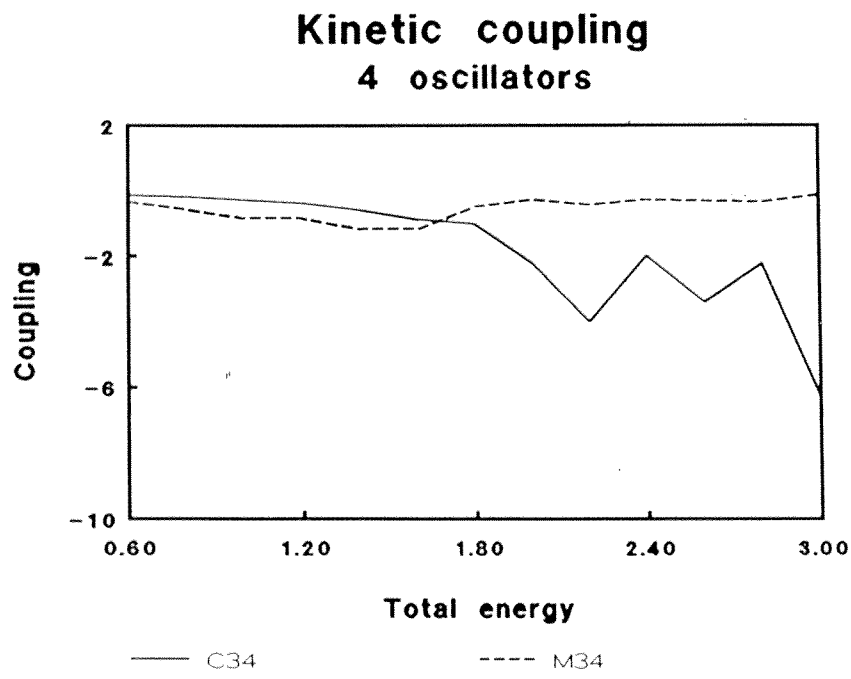

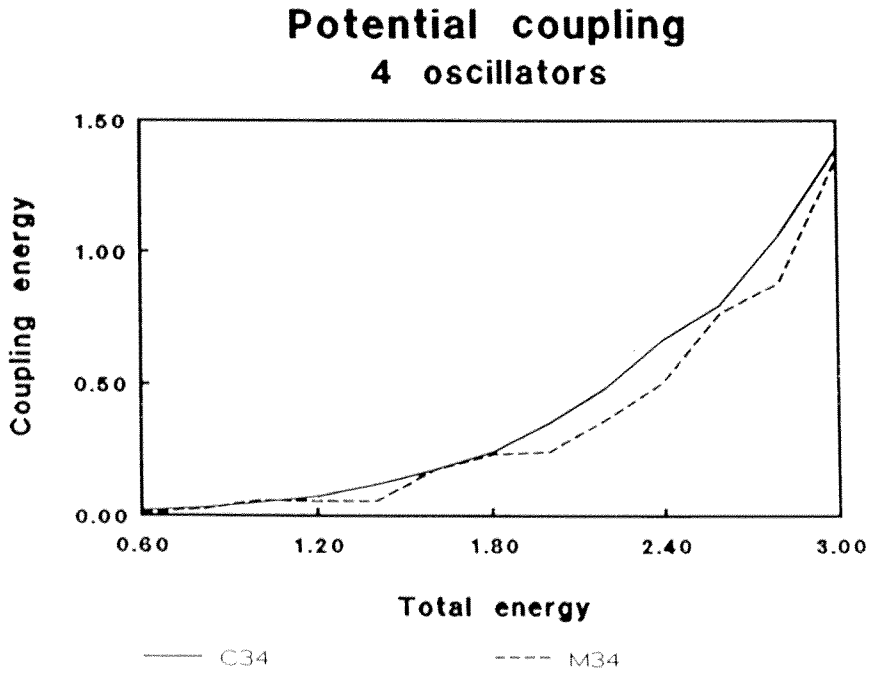

Şekil 4. Başlangıçta dengeden uzaklaştırılmış olan osilatörün komşusu ile olan ortalama kinetik ve potensiyel bağlantı terimlerinin, toplam enerji ile değişimleri.
Klasik mekanik ——————
Mixed-mode - - - - - -

Tr. J. of Physics
18 (1994) 1095 – 1105

Phase Space Representation of Wave Packets

P. Abdel JALIL, E. YURTSEVER
Middle East Technical University,
Department of Chemistry,
Ankara-TURKEY

Received 6.5.1994

Abstract

The phase space representation of quantum wave packets is discussed in terms of Husimi transformations. An algorithm of obtaining Husimi transforms of harmonic oscillator eigenfunctions is given and also applied to minimum uncertainty wavepackets as well as eigenfunctions of an anharmonic oscillator. Distributions of the Monte Carlo sampled classical points are compared to gain insight to the problem of phase space description of quantum mechanical problems.

1. Introduction

The history of the phase space representation in quantum mechanics extends back to the golden years of physics. However, the fundamental question of how to compare classical and quantum mechanical results, especially for dynamical problems, remains unanswered. Theoretically, there are an infinite number of ways to form phase space functions, but only two are in common practice: Wigner and Husimi transforms. Wigner's rule [1] states that for every quantum state a phase-space function can be defined according to

$$W(q,p) = \frac{1}{2\pi\hbar}\int_{-\infty}^{\infty} \Psi^*(q+x/2)\Psi(q-x/2)\exp(ixp/\hbar)dx \qquad (1)$$

where x is the coordinate in the quantum mechanical wavepacket and the p-q pair corresponds to classical momentum and coordinate. In eq (1) the Wigner transformation is defined for a one-dimensional wavepacket and generalization to many dimensional cases is straightforward. To set up the transformation, one constructs a numerical grid over p-q space; that is, for every (p,q) pair the intgral in eq. (1) is solved for the given wavepacket. This description has the correct asymptotic behavior and is always real valued, but it is necessarily negative in certain regions of the phase space. Since it is not

possible to interpret negative probability, the Wigner transform has conceptual difficulty in representing classical probability distribution [2]. However, it has been shown in some simple cases that Wigner function oscillates with a high frequency in the semiclassical limit; therefore, it can be smoothed out with a proper weight function [3]. Previous to this observation, Husimi has proposed that a Gaussian averaging would indeed yield a real and positive valued phase space representation [4].

$$\rho_H = \left| \int_{-\infty}^{\infty} \exp\left(-\frac{1}{w^2}(x-q)^2 + ipx \right) \Psi(x) dx \right|^2 . \tag{2}$$

Even though no rigorous answer exists to as why constructing Husimi transformations would provide a path between classical and quantum mechanical descriptions of a system, for the time being it seems to be the only available methodology [5-11].

2. Dynamical Systems

Our interest in this problem originates from our previous work on the comparison of classical dynamics and quantum description of two nonlinearly coupled oscillators [12-13]. We have shown that a classically chaotic system may display a more regular behavior in a quantum mechanical analysis. This regular behavior is in the form of eigenvalue statistics and nodal character of eigenfunctions which are all static properties. To have meaningful comparisons between two fundamentally different approaches, we have suggested a semiclassical mixed-mode approach [14-15]. In the self- consistent-field (SCF) approximation the total Hamiltonian of a two- dimensional system can be written as two separate one-dimensional operators and the nonlinear coupling is present in each equation in the form of average quantities. Let us define a nonlinear coupling in the form of x^2y^2, then the Hamiltonian is written as

$$H = H_x + H_y + \lambda x^2 y^2 \tag{3}$$

In SCF formalism we can write

$$\begin{aligned} H_x^{SCF} &= H_x + \lambda \langle y^2 \rangle x^2 \\ H_y^{SCF} &= H_y + \lambda \langle x^2 \rangle y^2 \end{aligned} \tag{4}$$

Here $\langle \cdots \rangle$ denotes an average potential over other modes. Dynamical equations involving these operators of either classical or quantal nature are then solved in an iterative manner. Let us assume that the motion along x coordinate is to be classical where the motion along y coordinate is quantal. The proper procedure to achieve this separation is to compare frequencies of each mode and to treat the slower mode classically as in the Born Oppenheimer approximation. The equations governing the dynamics of the problem can then be written as

whene $\chi_n(y) = N_n e^{-\frac{\alpha}{2}y^2} H_n(\sqrt{\alpha}y)$ is the harmonic oscillator eigenfunction with α^2 being the force constant.
If we define

$$f_n(p,q) = N_n \int_{-\infty}^{\infty} \exp\left[-\left(\frac{1}{w^2}+\frac{\alpha}{2}\right)y^2 + \left(\frac{2q}{w^2}+ip\right)y - \frac{q^2}{w^2}\right] H_n(\sqrt{\alpha}y)dy \qquad (11)$$

with

$$a = \left(\frac{2\alpha w^2}{2+\alpha w^2}\right)^{\frac{1}{2}}, b = \left(\frac{2+\alpha w^2}{2w^2}\right)^{\frac{1}{2}}, c = \frac{2q+ipw^2}{\sqrt{2w^2(2+\alpha w^2)}} \qquad (12)$$

we obtain [16]

$$f_n(p,q) = \frac{N_n}{b} e^{c^2 - \frac{q^2}{w^2}} \sqrt{\Pi}(1-\alpha^2)^{\frac{n}{2}} H_n\left(\frac{ac}{(1-a^2)^{\frac{1}{2}}}\right) \qquad (13)$$

which yields for ρ_H

$$\rho_H(p,q,t) = \sum_{n,m} c_m^*(t)c_n(t)\frac{N_n N_m 2w^2}{2+\alpha w^2}\Pi\left(\frac{2-\alpha w^2}{2+\alpha w^2}\right)^{\frac{(n+m)}{2}} \exp\left(\frac{p^2q^2+2\alpha q^2}{2+\alpha w^2}\right) \times$$
$$H_n(2q\lambda + ipw^2\lambda)H_m(2q\lambda - ipw^2\lambda) \qquad (14)$$

where $\lambda = \sqrt{\frac{\alpha}{4-\alpha^2 w^2}}$.
We have decided to look at two different types of wavepackets. In our previous mixed-mode calculations, we have employed the following anharmonic oscillator [12-14,17].

$$H_y = \frac{1}{2}p_y^2 + \frac{1.44}{2}y^2 - 0.0864y^3 - 0.002916y^4 \qquad (15)$$

Our one set of functions is chosen to be the eigenfunctions of the above Hamiltonian, which are usually written as linear combinations of basis functions (harmonic oscillator eigenfunctions):

$$\varphi_n = \sum_p c_{np}\chi_p \qquad (16)$$

This representation is more appropriate for spectroscopic studies since the initial states are usually expressed as combinations of adjacent eigenstates. We have also studied a minimum uncertainty wavepacket which is also known as the coherent state wavefunction. This Gaussian wavepacket is the closest representation to a classical point and it is the

most common choice for studying quantum dynamics. The expansion of a minimum uncertainty wavepacket in terms of harmonic oscillator eigenfunctions is given as [18]:

$$\Psi = \sum c_n \chi_n \tag{17}$$

where $c_n = \exp\left(-\frac{1}{2}\beta\right) \alpha^n \frac{1}{\sqrt{n!}}$ of which $\alpha = (x + ip), \beta = (x^2 + p^2)$, x and p are the coordinate and momentum.

3. Husimi Transforms

Since Husimi transformation of wavefunctions are functions of two variables, we choose to display them as surfaces on the p-q plane. In Figure 1 we present transformations of harmonic oscillator eigenfunctions for various quantum numbers. Except for the v=0 state, all have distorted ellipsoid shapes and zero magnitude at the center. This implies that any classical representation of these wavepackets should avoid the origin. When we look at the eigenfuctions of the anharmonic oscillator (Figure 2a-b), we see the anharmonicity with respect to the coordinate axis. For the minimum uncertainty wavepacket (Figure 2-c), the Husimi transform has the characteristics of a classical point with two peaks corresponding to a particle with same speed but opposite sign for momentum (same kinetic energy). Of course, in each case, widths of distribution functions depend on the weight factor of eq. (2).

In order to find the set of classical points for the given wavepacket, we have employed a Monte Carlo-like technique: an area on the p-q plane is defined such that the magnitude of the Husimi transform is practically zero outside. A random point within this range is selected and its probability of acceptance is defined as the value of the Husimi function at that point (Husimi probability function must be normalized). Then this probability is compared to a random number between 0 and 1 and if the probability is higher than the random number, the point is included in the set; otherwise, it is discarded.

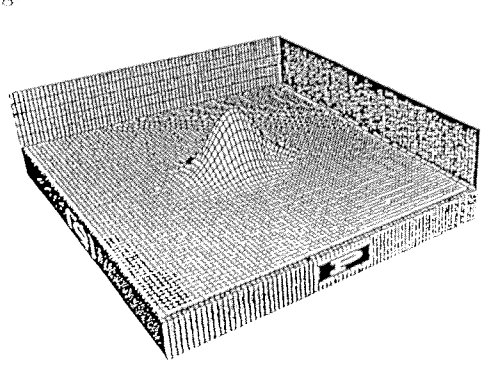

(a)

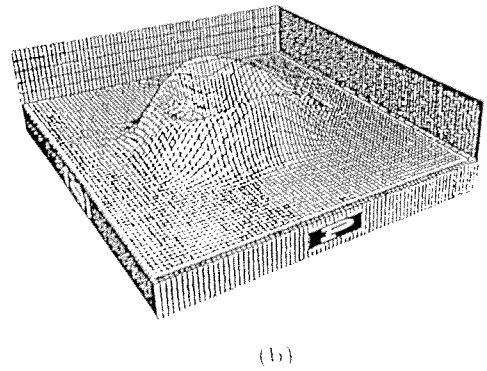

(b)

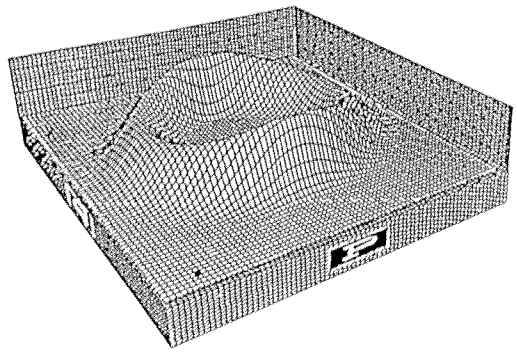

(c)

Figure 1. Husimi transformations of harmonic oscillator eigenfunctions. (a) v=0, (b) v=10, (c) v=20

Since the probability of being accepted becomes greater with higher Husimi function, we are able to generate a large number of points which should look like Husimi transforms. In Figure (3 and 4) we present 2-D histograms of 5000 points selected according to this procedure; these resemble the Husimi distributions.

These points are assumed to be the classical counterparts of the corresponding quantum wavepacket. Their distributions on the q-p plane resemble the Husimi transformations, however, with the basic difference that these points do not have the same classical energy. This point brings a different aspect to the problem compared to the standard method of the random selection of points along the constant Hamiltonian

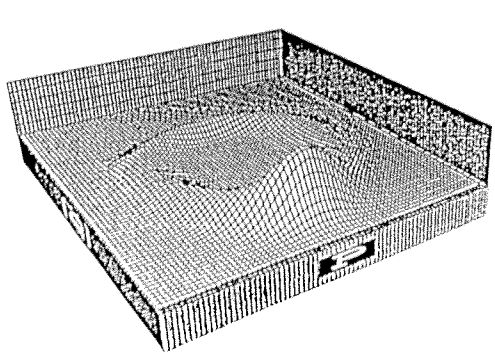

(a)

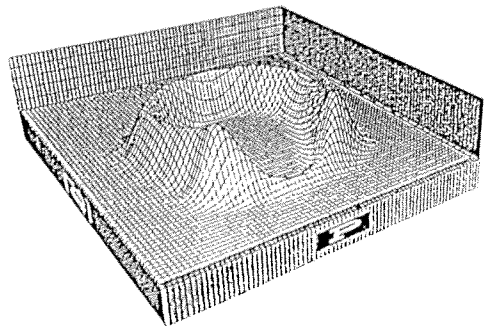

(b)

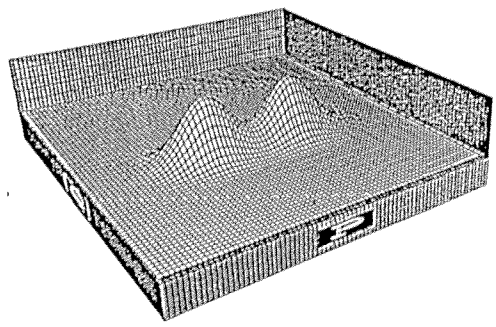

(c)

Figure 2. Husimi transformations of anharmonic oscillator eigenfunctions and a minimum uncertainty wavepacket. (a) anharmonic v=10, (b) anharmonic v=20, (c) minimum uncertainty wavepacket

Depending on the width of the Husimi weight factor, Monte Carlo points fall within an energy band. This appears to be the correct description for a probabilistic approach (quantum mechanics) where only the average values are discussed. For a qualitative observation, we have computed histograms of the distribution of these points on the energy scale (Figure 5 and 6). For the harmonic cases, we see the expected Gaussian shapes with maxima corresponding to the energy of the eigenfunction. Of course with an increasing number of points, the distributions become smoother. For the anharmonic eigenfunctions, shapes are Lorentzian as in the case of the minimum uncertainty wavepacket.

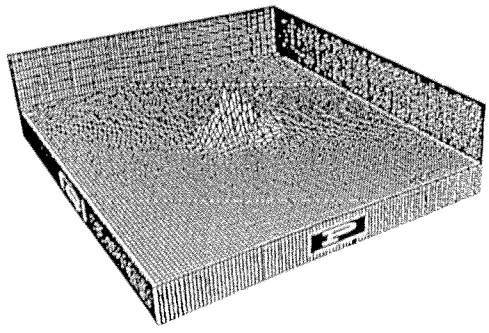

(a)

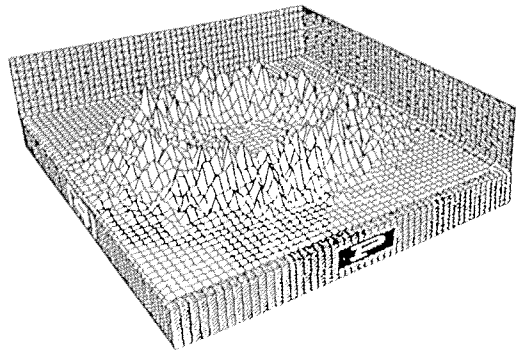

(b)

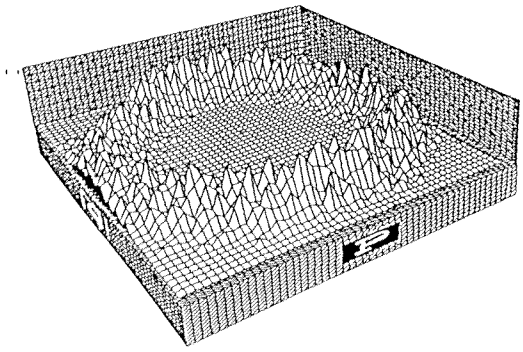

(c)

Figure 3. Monte Carlo weighed points from Husimi distributions of harmonic oscillator. (a) v=0, (b) v=10, (c) v=20

In all cases we observe points with very high and low energies which hopefully imply that such an ensemble may be the classical counterpart of the wavepacket. For example, it may be possible to model tunneling by classical mechanics even though tunneling is a quantum mechanical phenomenon.

In this work we have presented formulas for Husimi transforms of harmonic oscillator eigenfunctions. We have used a Monte Carlo method to select classical points which would be the corresponding set for the quantum wavepacket. Distributions of these points on the energy scale are given for various harmonic and anharmonic functions. Now the next step is to attempt to answer the question of whether the Husimi weighed points for different wavepackets display different classical behavior.

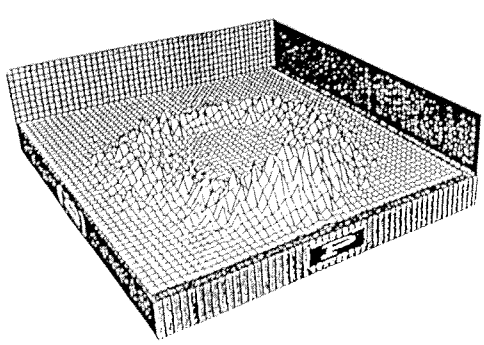

(a)

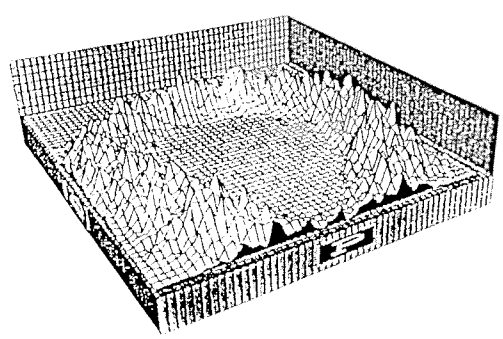

(b)

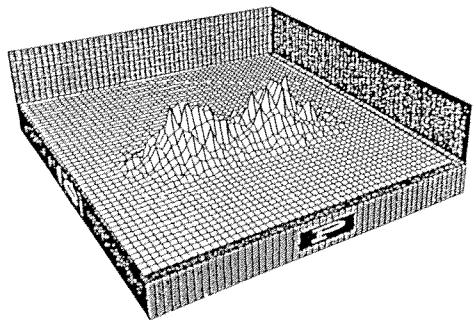

(c)

Figure 4. Monte Carlo weighed points from Husimi distributions of the functions in Figure 2 (a) anharmonic v=10, (b) anharmonic v=20, (c) Minimum uncertainty wavepacket

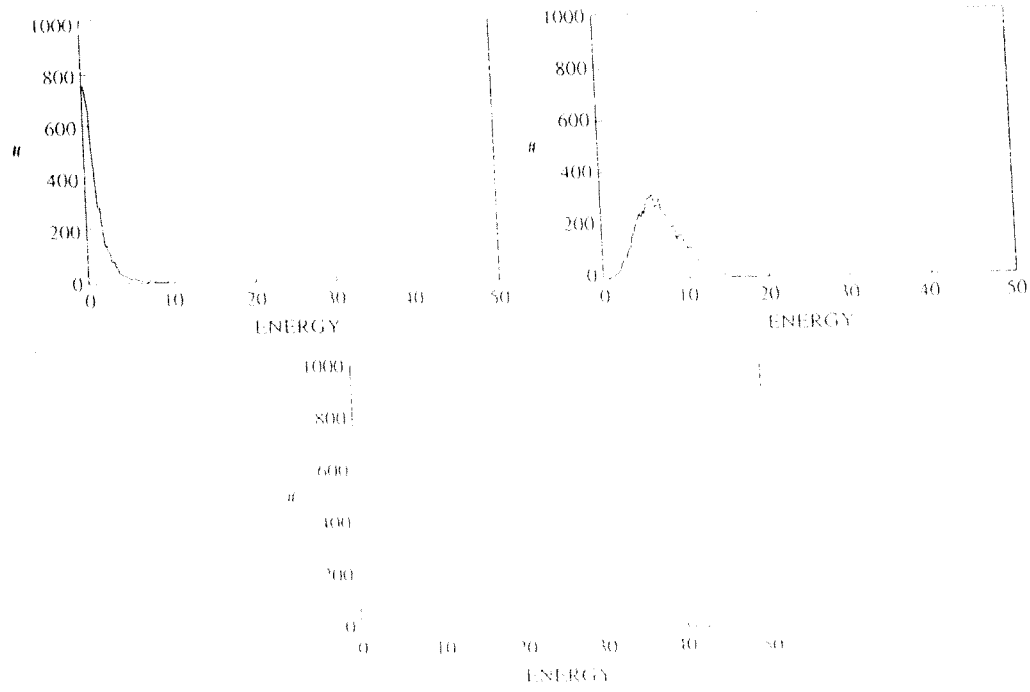

Figure 5. Energy distribution of the points from Figure 3

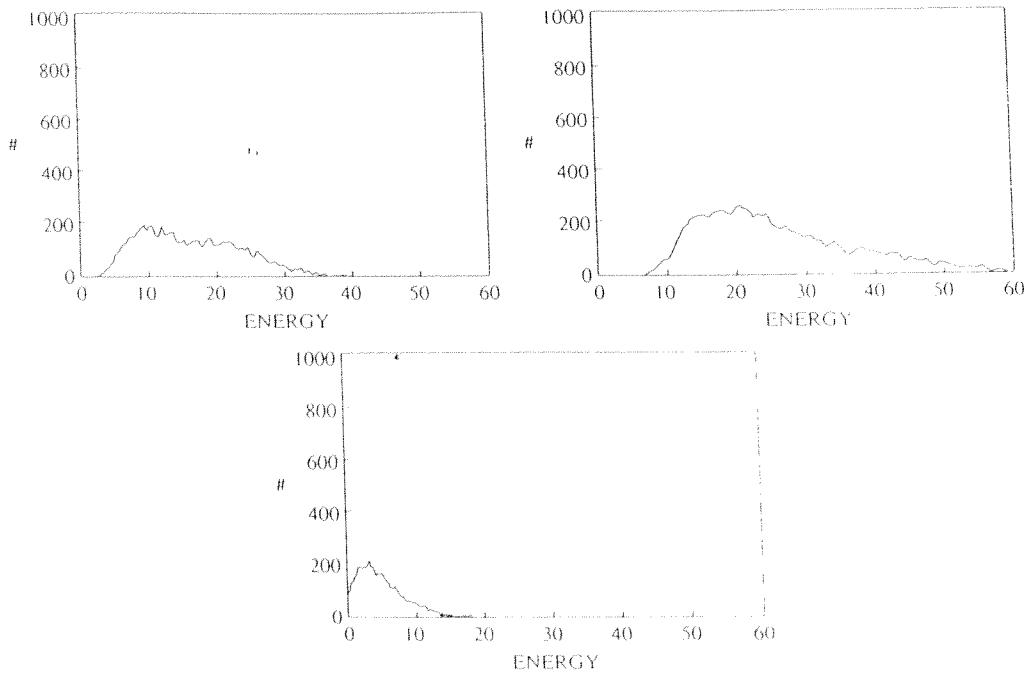

Figure 6. Energy distribution of the points from Figure 4

We are in the process of computing Lyapunov exponent spectra for a two-dimensional system for sets of initial points selected from different wavepackets. The variation of the chaotic behaviour of these sets hopefully would give us some clues for the classification of quantum wavepackets.

Acknowledgements

We would like to acknowledge that this project has been supported by TUBITAK with the project TBAF-1218 and by the NATO grant GRG 900087

References

[1] E. P. Wigner, *Phys. Rev.*, **40**, 749-759 (1932)

[2] W. Zurek, *Physics Today, October*, 36-44 (1991)

[3] R. E. de Carvalho and M. A. M. De Aguiar, *Phys. Rev. A*, **46**, 1128-1131 (1992)

[4] K. Husimi, *Proc. Phys. Math. Soc. Japan*, **22**, 264-313 (1940)

[5] K. Takahashi and N. Saito, *Phys. Rev. Lett.*, **55**, 645-648 (1985)

[6] K. Takahashi, *J. Phys. Soc. Japan*, **55**, 762-779 (1986).

[7] K. Zyckowski, *Phys. Rev A*, **35**, 3546-3549 (1987).

[8] J. E. Harriman, *J. Chem. Phys.*, **88**, 6339-6408 (1988).

[9] G. J. Milburn, *Phys. Rev. A*, **39**, 2749-2750 (1989).

[10] F. Borondo, "Computational Chemistry: Structure, Interactions and Reactivity", Ed. S. Fraga, Vo. 77, 592-620 (1992).

[11] J. E. Harriman and M. E. Casida, *Int. J. Quant. Chem.*, **45**, 263-294 (1993).

[12] E. Yurtsever and J. Brickmann, *Phys. Rev. A*, **41**, 6688- 6691 (1990).

[13] E. Yurtsever and J. Brickmann, Berichte der Bunsenges, *Phys. Chem.*, **94**, 804-827 (1992).

[14] E. Yurtsever and J. Brickmann, Berichte der Bunsenges, *Phys. Chem.*, **96**, 142-146 (1992).

[15] E. Yurtsever and T. Uzer, Berichte der Bunsenges, *Phys. Chem.*, **94**, 906-913 (1992).

[16] I. S. Gradshteyn and I. M. Ryzhik, "Tables of Integrals, Series and products", academic Press, p. 837 (1965).

[17] E. Yurtsever "Integrability and Chaotic Behaviour", ed. J. Seimenis Kluwer Press (In Press).

[18] J. Brickmann, *J. Chem. Phys.*, **78**, 1884-1894 (1983).

Hamilton-Jacobi Dynamics for the Solution of Time Dependent Quantum Problems I. Formalism and Wave Packet Propagation in One Dimension

Ersin Yurtsever

Middle East Technical University, Department of Chemistry, Ankara, Turkey

Jürgen Brickmann*)

Technische Hochschule Darmstadt, Physikalische Chemie I, Petersenstr. 20, D-64287 Darmstadt, Germany

Key Words: Computer Experiments / Quantum Mechanics / Wave Functions

Two methods for the numerical integration of the time-dependent Schrödinger equation with given initial conditions (initial wave packet) are presented. The first method (method A) is based on the Schrödinger representation of the quantum-dynamical system while the second one (method B) is based upon the intermediate representation. In both cases the quantum dynamical equation is transformed into a system of Hamilton-Jacobi type equations of motion as occurring in multi particle classical dynamics, i.e. standard molecular dynamics techniques can be applied for the integration. The dynamics of a minimum uncertainty Gaussian wave packet in a strongly anharmonic oscillator is taken as an example.

1. Introduction

In molecular science there are many phenomena for which the time evolution of observable properties can only be adequately described within the framework of quantum mechanics. Examples are all processes where tunneling plays a dominant role (like proton transfer reactions or electron transfer between different microscopic system) or those phenomena where phase correlations become important (like all types of induced transitions between atomic or molecular states) [1]. All methods dealing with the integrations of time dependent quantum mechanical problems are based on the solution of the time dependent Schrodinger equation[1])

$$i\frac{\partial|\varphi\rangle}{\partial t} = H|\varphi\rangle \quad . \tag{1.1}$$

The exact solution of this equation is only possible for a very limited number of physical systems. Examples are those where the time independent Schrodinger equation

$$H|\varphi_i\rangle = E_i|\varphi_i\rangle \tag{1.2}$$

with a stationary Hamiltonian H can be solved or when the time dependent states remain "coherent" [2 – 6]. In the first case an arbitrary initial wave packet φ_0 can be expanded with respect to the eigenfunctions of this Hamiltonian as

$$|\varphi(t)\rangle = \sum_v c_v(t)|\varphi_v\rangle \tag{1.3}$$

with

$$c_v(t) = \exp(-iE_v t)c_v(0) \quad . \tag{1.4}$$

The expansion coefficients $c_v(t)$ are determined for all times. If the eigenfunctions of H are only approximately known then Eq. (1.3) represents only an approximation of the exact solution but the formalism is the same. Traditionally, the determination of approximate solutions of Eq. (1.2) is equivalent to the diagonalization of a Hermitean matrix. This method works well for small and simple systems but becomes uneffective for complex large systems, particularly when massively parallel computer technology is applied [1]. For time dependent Hamiltonians this method fails in general.

There are more effective procedures to solve Eq. (1.2) which use finite difference techniques [1]. Through the introduction of Fourier methods [1] and using fast Fourier transform techniques a grid based technology can be applied which is particularly useful when massively parallel computers are used.

The motivation for the present work is not related to any need for another algorithm to integrate the time dependent Schrodinger equation, but to establish a formalism which allows the treatment of multi-dimensional molecular systems in such a way, that some degrees of freedom of a molecular system (typically vibrational manifolds) can be treated quantum mechanically but that the majority of degrees of freedom can be treated classically and coupled to the "relevant" degrees in some way. A typical coupling approach is based on the time dependent self consistent field approximation discussed by Gerber, Raynet and coworkers [7].

Consequently, the method we have in mind should fulfill the following requirements. It should

(1) work well even for large systems, i.e. there should not be any restriction, which is related to the maximum size of matrices, which can be diagonalized.

*) Author to whom correspondence should be addressed.

[1]) Here and in the following generalized coordinates are always used, i.e. frequencies are measured as multiples of ω_0, energies are measured as multiples of $\hbar\omega_0$, time is measured in units of ω_0^{-1}, positions are measured as multiples of $[m\omega_0\hbar]^{-1/2}$, momenta are measured in units of $[m\omega_0\hbar]^{1/2}$, where m is the mass of the particle, ω_0 is the angular frequency of a basic oscillator, and $\hbar$ is Planck's constant devided by 2π.

 VCH Verlagsgesellschaft mbH, D-69451 Weinheim, 1994 0005-9021/94/0404-0554 $ 10.00+.25/0

(ii) be extendable to time dependent SCF procedures [7],
(iii) be extendable to classical quantum mixed mode problems [7–9],
(iv) and be transferable to massively parallel computer systems [1].

In this paper we only present the formalism and the results of some model calculations and some benchmarks. In order to work effectively even for large systems we followed two lines of thought. One (method A) is based on the Schrödinger representation while the other (method B) begins at the intermediate representation [10]. In both cases a formal transformation of the time dependent Schrödinger equation (1.1) to Hamilton-Jacobi type equations of motion for formal position- and momentum-coordinates is performed and these equations are solved numerically with technology of the molecular dynamics type. In Chap. 2 the formal work is described, while in Chap. 3 some numerical results for the dynamics of an initially minimum uncertainty Gaussian wave packet are presented. In the final Chap. 4 some conclusions are drawn and an outlook on future applications is given.

2. Formalism

2.1 Schrödinger Representation

Since we are basically interested initially in the time development of given wave packets, the Schrödinger representation [10] is the most convenient one because of the fact that in this representation all the time dependence is (for stationary Hamiltonians) focused on the wave functions.

Starting with a Hamiltonian

$$H = H_0 + V \tag{2.1}$$

where H_0 is Hamiltonian for which the eigenfunctions φ_k are known and V is a perturbation which does not necessarily have to be small, the time dependent Schrödinger Eq. reads

$$\mathrm{i}\frac{\partial|\varphi\rangle}{\partial t} = H|\varphi\rangle \ . \tag{2.2}$$

Expanding φ formally with respect to the basis functions gives

$$|\varphi\rangle = \sum_i c_i|\varphi_i\rangle \tag{2.3}$$

We follow the arguments of Manz [11] and substitute

$$x_v = \mathrm{Re}(c_v) \ , \quad p_v = \mathrm{Im}(c_v) \tag{2.4}$$

into Eq. (2.2) and multiplying from the left with $\langle\varphi_u|$ results in

$$\mathrm{i}(\dot{x}_u + \mathrm{i}\dot{p}_u) = \sum_v (x_v + \mathrm{i}p_v)H_{uv} \quad \text{with} \quad H_{uv} = \langle\varphi_u|H|\varphi_v\rangle \ . \tag{2.5}$$

We write the matrix elements of the Hamiltonian in the form

$$H_{uv} = a_{uv} + \mathrm{i}b_{uv} \tag{2.6}$$

where a_{uv} and b_{uv} are elements of real symmetric matrices, i.e.

$$a_{uv} = a_{vu} \ , \quad b_{uv} = b_{vu} \ . \tag{2.7}$$

From the real and the imaginary part of Eq. (2.5) it results that

$$\frac{\partial x_u}{\partial t} = \sum_v [p_v a_{uv} + x_v b_{uv}] \tag{2.8}$$

and

$$\frac{\partial p_u}{\partial t} = -\sum_v [x_v a_{uv} - p_v b_{uv}] \ . \tag{2.9}$$

We define a formal Hamiltonian as

$$H = \frac{1}{2}\sum_{u,v}(x_u - \mathrm{i}p_u)(x_v + \mathrm{i}p_v)H_{uv} \ . \tag{2.10}$$

Immediately we see that

$$\frac{\partial H}{\partial x_u} = \sum_v (x_v a_{uv} - p_v b_{uv}) \tag{2.11}$$

and

$$\frac{\partial H}{\partial p_u} = \sum_v (p_v a_{uv} + x_v b_{uv}) \ . \tag{2.12}$$

Consequently

$$\frac{\partial x_u}{\partial t} = \frac{\partial H}{\partial p_u} \ , \quad \frac{\partial p_u}{\partial t} = -\frac{\partial H}{\partial x_u} \tag{2.13}$$

which are the Hamilton-Jacobi equations of motion for a classical oscillator in n dimensions [11] with the momentum- and position component p_u and x_u, i.e. we have reduced the approximate solution of the time dependent Schrödinger Eq. (1.1) to a problem which can be treated with methods commonly used in classical dynamics.

It should be noted here that Eq. (2.13) is also valid when the physical problem under consideration is not stationary, i.e. if the Hamiltonian H is explicitly time dependent. However, one cannot say anything on the stability of the solution without considering the explicit form of the perturbation.

For time independent Hamiltonians the dynamics of the whole system are linear, i.e. all n-dimensional trajectories

are expected to be stable. For this latter case one can take the conservation of the energy to be:

$$E = \langle H \rangle = \sum_{uv} (x_u - ip_u) H_{uv} (x_v + ip_v) \tag{2.14}$$

and the conservation of the norm to be:

$$\sum_v [x_v^2 + p_v^2] = 1 \tag{2.15}$$

as criteria for the quality of the numerical procedure.

2.2 Intermediate Representation

The intermediate representation [10] is useful for all cases where the model system can be split in a way such that the fast motion, which may be related to the action of the zero order Hamiltonian H_0, can be transformed out of the equation of motion. Such a separation may be very useful in order to make numerical procedures more effective. In this work we also have used this representation to test how explicit time dependence of an effective Hamiltonian is influencing the stability of numerical integration procedures.

In the intermediate representation the time evolution of a wave packet φ_I is determined by [10]

$$i \frac{\partial |\varphi_I\rangle}{\partial t} = V_I |\varphi_I\rangle \tag{2.16}$$

with the perturbation Hamiltonian

$$V_I = U_0^+ V U_0 \tag{2.17}$$

and the time evolution operator for the zero order motion

$$U_0 = \exp(-iH_0 t) \ . \tag{2.18}$$

Again we expand the wave vector φ_I as a linear combination of the eigenstates of the zero order Hamiltonian

$$|\varphi_I\rangle = \sum_v (x_v + ip_v) |\varphi_v\rangle \tag{2.19}$$

and interpret the x- and p-components as position- and momentum components occurring in a Hamiltonian as

$$H_I = \frac{1}{2} \sum_{u,v} (x_u - ip_u)(x_v + ip_v)(V_I)_{uv} \tag{2.20}$$

with time dependent contributions

$$(V_I)_{uv} = \exp[i(\varepsilon_u - \varepsilon_v)t] \langle \varphi_u | V | \varphi_v \rangle \ . \tag{2.21}$$

With the Hamiltonian Eq. (2.20) the equations of motion for the formal position- and momentum components are identical to those of the Schrödinger representation (see Eq. (2.13)).

2.3 Newton's Equation of Motion

As has been mentioned above, the formalism presented here should be used in mixed classical quantum calculations within the scheme of a time dependent SCF procedure. Since the numerical integration of the classical motion in most cases (for example in most molecular dynamics algorithms like the Verlet scheme [14]) does not start from Hamilton-Jacobi type equations of motion but from Newton's equation of motion, it is reasonable to use this type of numerical integration scheme also for the quantum motion. A transformation to Newton's type of equation is easily possible for the formalism based on the Schrödinger representation (see Sect. 2.1) at least in those cases where the Hamiltonian is not explicitly time dependent. From Eqs. (2.8) and (2.9) one obtains

$$\frac{\partial^2 x_u}{\partial t^2} = \sum_w \sum_v [-a_{uv} a_{vw} + b_{uv} b_{vw}] x_w + \sum_w \sum_v [a_{uv} b_{vw} + b_{uv} a_{vw}] p_w \tag{2.22}$$

and

$$\frac{\partial^2 p_u}{\partial t^2} = \sum_w \sum_v [-a_{uv} b_{vw} - b_{uv} a_{vw}] x_w + \sum_w \sum_v [-a_{uv} a_{vw} + b_{uv} b_{vw}] p_w \tag{2.23}$$

i.e. if the Hamiltonian is represented by a real symmetric matrix $H_{uv} = a_{uv}$, Newton's equations of motion read

$$\frac{\partial^2 x_u}{\partial t^2} = -\sum_w \left| \sum_v a_{uv} a_{vw} \right| x_w \tag{2.24}$$

and

$$\frac{\partial^2 p_u}{\partial t^2} = -\sum_w \left| \sum_v a_{uv} a_{vw} \right| p_w \tag{2.25}$$

which both can be integrated with standard MD procedures for multi particle systems using, for example, the Verlet scheme [14].

3. Wave Packet Dynamics in One Dimension

3.1 Model Systems

In order to test the formalisms presented in Sect. 2, various numerical calculations have been performed with a harmonic oscillator coherent state (HOCS) [2, 6] as an initial wavepacket moving in a one dimensional strongly anharmonic potential [9]. The zero order Hamiltonian is chosen to be harmonic

$$H_0 = \frac{1}{2}[P^2 + X^2] \tag{3.1}$$

while for the anharmonic perturbation

$$V(X) = -0.05X^3 + 0.00140625X^4 \tag{3.2}$$

is used. The complete potential $X^2/2 + V(X)$ has a single minimum at $X = 0$ and a plateau value ($V' = 0$, $V'' = 0$) for an energy of $V = 15$.

The expansion coefficients of a HOCS, located initially at

$$X(t = 0) = X_0 = 5.5 \ , \quad P(t = 0) = P_0 = 0 \tag{3.3}$$

with respect to the eigenstate of an harmonic oscillator with the angular frequency $\omega = 1$, can be analytically given as [2, 3]

$$c_k = \exp(-\tfrac{1}{2}|\alpha|^2)\alpha^k(k!)^{-1/2} \tag{3.4}$$

with

$$\alpha = 2^{-1/2}(X + iP) \ . \tag{3.5}$$

Three independent series of calculation have been performed:

(a) The eigenfunctions of the complete Hamiltonian have been determined within the variational scheme using, as a basis, n harmonic oscillator eigenfunctions of the zero order Hamiltonian. The time evolution of the initial HOCS is calculated in accordance with Eq. (1.3) with the coefficients of Eq. (1.4). The largest size of the basis sets used here was $n = 75$. The maximum basis size was chosen such that the expansion coefficients of the initial wave packet (with respect to the approximate eigenfunction function with the highest quantum number) did not exceed a value of 10^{-6}. The solution of Eq. (1.1) in this approximation is taken as a reference in the following and is termed "exact".

(b) The time propagation of the expansion coefficients has been determined numerically based on the Schrodinger representation by integrating Hamilton-Jacobi equations of motion Eq. (2.14) with a Runge-Kutta integration scheme by using different time steps

$$10^{-2} \geq \Delta t \geq 10^{-5} \tag{3.6}$$

(measured in ω^{-1} units).

(c) The time propagation of the expansion coefficients has been determined numerically on the basis of the intermediate representation as in (b) where now the matrix elements Eq. (2.21) of the Hamiltonian have the form

$$(V_I)_{uv} = e^{i(u-v)t}\langle u|V(X)|v\rangle \tag{3.7}$$

where $|v\rangle$ are the eigenstates of the zero order harmonic Hamiltonian Eq. (3.1)

$$H_0|v\rangle = (v + \tfrac{1}{2})|v\rangle \ . \tag{3.8}$$

3.2 Numerical Results

We have chosen an initial wave packet φ_0 with P_0- and X_0-values such that the total energy results as

$$E = \langle\varphi_0|H_0 + V|\varphi_0\rangle = 12.04 \ . \tag{3.9}$$

For this energy the anharmonicity of the potential function generates a fast decay of the wave packet, i.e. φ remains coherent only within a time scale which is comparable to a classical oscillation period [12]. The real and imaginary parts of the wave function φ – as obtained from the "exact" solution (a) – are drawn in Fig. 1.

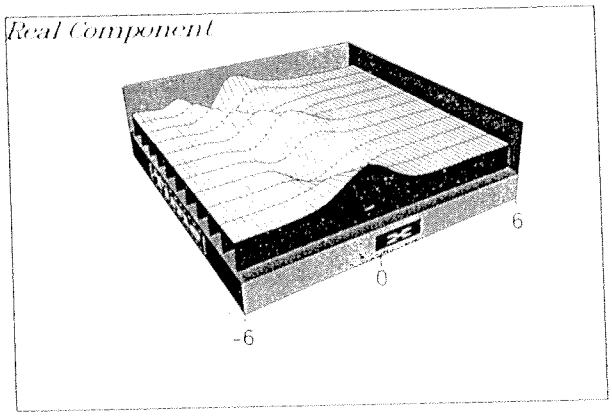

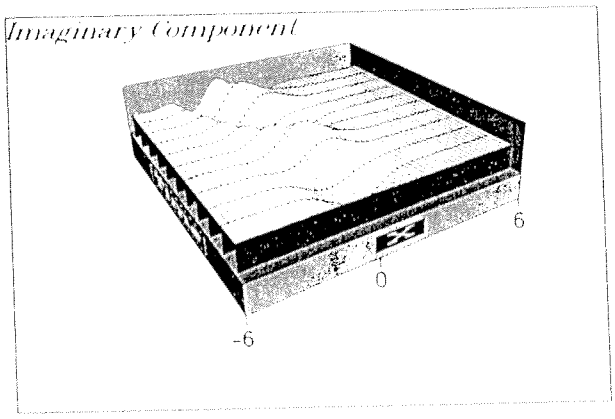

Fig. 1
Time evolution of the real and imaginary part, (a) and (b), respectively, of an initially minimum uncertainty wave packet with initial energy $E = 12.04$ as obtained from the "exact" solution $\varphi_{exact}(t)$ of the time dependent Schrodinger equation for a time period of $t = 0 \ldots$

The accuracy of the numerical solutions (b) and (c) can be measured by considering the overlap between the "exact" wave packet φ_{exact} and the approximated one φ_{appr}

$$\langle\varphi_{exact}|\varphi_{appr}\rangle = \sum_v |c_v(t) - c'_v(t)| \tag{3.10}$$

We have calculated the quantity

$$\delta = (1 - \langle\varphi_{exact}|\varphi_{appr}\rangle)^2 \tag{3.11}$$

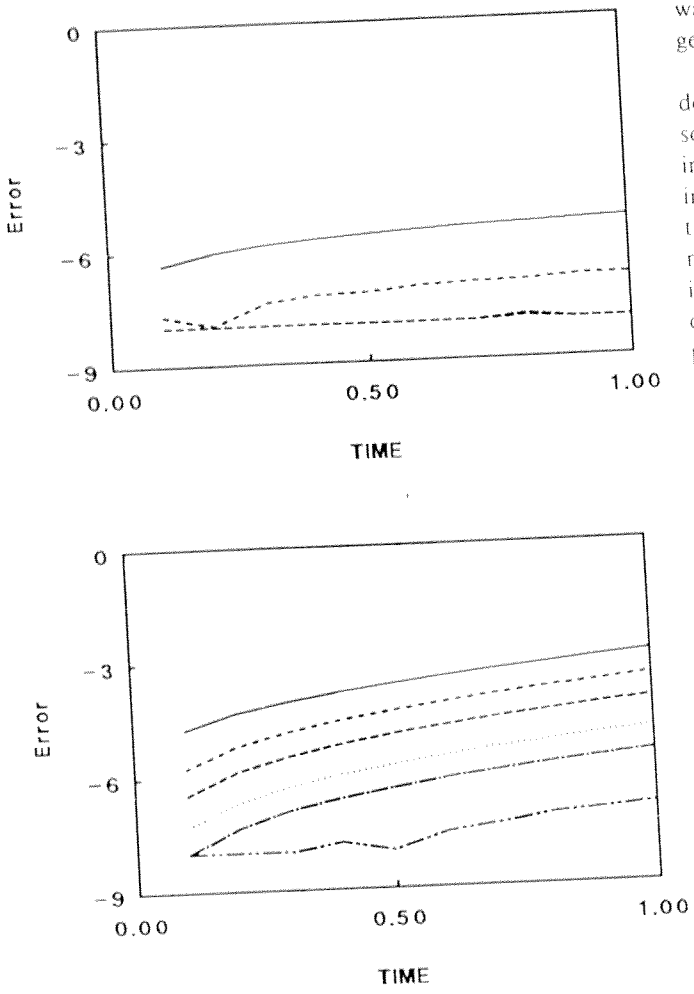

Fig. 2
Logarithm of the numerical error (ERROR = $_{10}\log(\delta)$, see Eq. (3.11)) against time for the numerical integration of the dynamic equation based on the Schrödinger (a) and the intermediate representation (b) for different integration time steps: $\Delta t = 0.01$ (————), $\Delta t = 0.05$ (– – –), $\Delta t = 0.0025$ (— — —), $\Delta t = 0.001$ (· · · · · ·), $\Delta t = 0.0005$ (— · — · —), and $\Delta t = 0.0001$ (— · · — · · —); all in units of ω^{-1}. The time is given in $0.01\ \omega^{-1}$ units

as a measure of the deviation of both. In Fig. 2 the logarithm of this error measure is plotted against time, where different integration time steps have been used in the numerical procedures.

It is seen from these figures that, for the present model system and the selected initial conditions, the results obtained on the basis of the Schrödinger representation are more accurate than those obtained with the intermediate scheme. Even for a time step of $\Delta t = 0.01\ \omega^{-1}$ the δ-values do not exceed 10^{-6} substantially in the Schrödinger type case. For $\Delta t \leq 0.0025$ the δ-values do not depend any longer on the magnitude of the integration time step.

The higher sensitivity of the results in the intermediate case is obviously related to the occurrence of high frequency terms in the effective Hamiltonian Eq. (3.7). These terms do not become small since in the energy range of the initial wave packet the strong anharmonicities of the potential generate large nondiagonal terms in Hamiltonian.

The numerical efforts for the determination of the time dependent coefficients $c_\nu(t) = x_\nu(t) + ip_\nu(t)$ for the "exact" solution and the Schrödinger representation type approximation (b) are of comparable magnitude, i.e. the approximations described above are not faster in the present case than the diagonalization technique. However, the memory requirements are much less in the difference techniques used in the approximations (b) and (c) than in the matrix diagonalization method (a). This fact is definitely not important for the model case studied in this paper, since the number of basis functions is small, but it becomes important for large systems where 10^4 to 10^6 basis functions will be required for reasonable accuracy of the expansion coefficients.

4. Conclusions

It has been demonstrated that the time dependent Schrödinger equation can be effectively solved by introducing formal position- and momentum-coordinates and transforming this equation to a Hamilton-Jacobi type set of equations of motion, which then can be treated by techniques known from molecular dynamics simulation treatments. Two different schemes have been introduced, one based on the Schrödinger representation and one on the intermediate representation of quantum states and operators [10]. For time independent Hamiltonians (i.e. systems where the time dependent expansion coefficient can be directly obtained from the solutions of the time independent Schrödinger equation – at least in principle) the numerical procedure (method A) is very stable, because the equations of motion become all linear with constant coefficients. The conservation of energy and the conservation of the norm can be taken as criterions for the stability of the solution (as is done in molecular dynamics treatments). The method based on the intermediate representation (method B) is less numerically stable, at least for the numerical example treated in this work. However, this method can be applied also to systems, where the Hamiltonian becomes explicitly time dependent and possible high frequency terms can be transformed out before starting the numerical procedure.

The present investigation was not motivated by the necessity to add an additional procedure to the variety of approximative strategies for the solution of time dependent quantum problems (see for a review Ref. [1] and [13]) but to test a formalism which is particularly useful for the treatment of mixed classical-quantum systems [7–9, 15]. For example, the treatment of two quantum degrees of freedom (with N basis function considered) coupled to M classical degrees of freedom in a time dependent self consistent field manner [7] leads to an $N+M$ dimensional classical system of Newton's equations of motion, which can be treated with molecular dynamics simulation type techniques in a very effective way. This will be demonstrated in paper II of this series [15].

This work has been supported by the Deutsche Forschungsgemeinschaft, Bonn, the Volkswagenstiftung, Hannover, and TÜBITAK, Ankara (TBAG-1218). We would like to thank an anonymous referee for reading this manuscript carefully.

References

[1] See for a review: R. Kosloff, J. Phys. Chem. *92*, 2087 (1988).
[2] (a) R.J. Glauber, Phys. Rev. *130*, 2529 (1963); *131*, 2766 (1963), Phys. Lett. *21*, 650 (1966).
(b) E.H. Kerner, Can. J. Phys. *36*, 371 (1958).
[3] P. Caruther and M.M. Nieto, Am. J. Phys. *33*, 537 (1965).
[4] (a) C.C. Gerry, Phys. Rev. *a33*, 2148 (1986).
(b) C.L. Mehta and E.C.G. Sudarshan, Phys. Lett. *23*, 574 (1966).
[5] R. Marquardt and M. Quack, J. Chem. Phys. *90*, 6320 (1989).
[6] J. Brickmann and P.C. Schmidt, Int. J. Quantum Chem. *23*, 47 (1983).
[7] (a) R.B. Gerber, V. Buch, and M.A. Ratner, J. Chem. Phys. *77*, 3022 (1982);
(b) R.B. Gerber and M.A. Ratner, Adv. Chem. Phys. *70*, 97 (1988).
[8] E. Yurtsever and T. Uzer, Ber. Bunsenges. Phys. Chem. 1993.
[9] E. Yurtsever and J. Brickmann, Ber. Bunsenges. Phys. Chem. *96*, 142 (1992).
[10] A. Messiah, "Quantum Mechanics", pp. 310–323, Vol. 1, North Holland Publ. Co., Amsterdam, 1961.
[11] J. Manz, J. Chem. Phys. *91*, 2190 (1989).
[12] (a) J. Brickmann, J. Chem. Phys. *78*, 1984 (1982);
(b) J. Brickmann and P. Russegger, Chem. Phys. Lett. *89*, 239 (1982);
(c) J. Brickmann and P. Russegger, Chem. Phys. *68*, 369 (1982).
[13] For a review of wave packet dynamics see: E.J. Heller in "Chaos and Quantum Physics" pp. 1–134, Nato Lectures, eds. by A. Voros, M. Gianonni, O. Bohigas, North Holland Publ. 1990.
[14] L. Verlet, Phys. Rev. *159*, 98 (1967).
[15] Th. Gunkel, M.C. Engel, E. Yurtsever, and J. Brickmann, to be published.

(Received: September 6, 1993
final version: December 20, 1993)

E 8476

Hamilton-Jacobi Dynamics for the Solution of Time Dependent Quantum Problems II. Wave Packet Propagation in Two Dimensional, Nonlinearly Coupled Oscillators – Exact and Time-Dependent SCF-Solutions –

Thomas Gunkel[a], Hans-Jürgen Bär[a], Michael Engel[b], Ersin Yurtsever[c], and Jürgen Brickmann[a]*)

[a] Technische Hochschule Darmstadt, Physikalische Chemie I, Petersenstr. 20, D-64287 Darmstadt, Germany

[b] Center for Visualization of Dynamic Systems, Hebrew University, Jerusalem, Israel

[c] Middle East Technical University, Department of Chemistry, Ankara, Turkey

Key Words: Computer Experiments / Quantum Mechanics / Wave Functions

Methods for the approximate numerical integration of the time dependent Schrödinger equation with given initial conditions (the initial wave packet) are presented. The methods are based on the Schrödinger representation of the quantum dynamic system. The quantum dynamic equations are transformed into Hamilton-Jacobi type equations of motion as they occur in multi particle classical dynamics, i.e. standard techniques in molecular dynamics can be applied for the integration. The dynamics of minimum uncertainty Gaussian wave packets in strongly nonharmonic, nonlinearly coupled oscillators are studied as examples. The numerically exact solutions are compared to time dependent SCF approximations of the wave packet.

I. Introduction

In a recent work of two of the authors [1] (referred to as paper I in the following text) it has been demonstrated that the time dependent Schrödinger equation[1])

$$i\frac{\partial|\varphi\rangle}{\partial t} = \hat{H}|\varphi\rangle \tag{1.1}$$

for the dynamics of a wave packet in one-dimensional, bound systems can be effectively solved by introducing formal position – and momentum – coordinates and transforming this equation to Hamilton Jacobi or Newton type sets of equations of motion which can then be treated with techniques already known from molecular dynamics simulation treatments. Two different schemes have been introduced in paper I, one based on the Schrödinger representation and one on the intermediate representation of quantum states and operators [2]. For time independent Hamiltonians (i.e. systems where the time dependent expansion coefficient can in principle be directly obtained from the solution of the time independent Schrödinger equation) the numerical procedure is very stable, because the equations of motion all become linear and with constant coefficients. The conservation of energy and the conservation of the norm can be taken as criteria for the stability of the solution and is analogous to treatments in molecular dynamics. The method based on the intermediate representation is less numerically stable; at least for the numerical example treated in paper I. However, the latter method can be applied also to systems where the Hamiltonian becomes explicity time dependent and possible high frequency terms can be transformed out before starting the numerical procedure.

In the present investigation the dynamics of a two-dimensional wave packet in a strongly anharmonic, nonlinearly coupled oscillator system is studied. In this case only bound states have to be considered in the basis set and all formal coupling terms are real quantities. Two different approaches are considered:

(i) The expansion of the time dependent wave packets with respect to a basis of products of one-dimensional zero order eigenstates, i.e. eigenstates of one-dimensional, nonlinear oscillators, and

(ii) The evolution of the initial wave packet within the time dependent SCF approximation, whereby the dynamic along one coordinate is determined by the mean field generated by the wave packet moving along the second coordinate and vice versa.

In both cases the Schrödinger Eq. (1.1) is transformed into a set of equations of motion of Newton's type.

In section II the transformations of the quantum equations into classical equations of motion are shortly reviewed whilst section III deals with the time dependent SCF approach. In section IV, the analytical treatment of the "exact" solution as well as of the TDSCF method is described. The results of numerical calculations on the time evolution of wave packets in a two dimensional oscillator system are presented in section V. Some conclusions are drawn in the final section VI.

*) Author to whom correspondence should be addressed.

[1]) Here and in the following equations generalized coordinates are always used, i.e. frequencies are measured as multiples of ω_0, energies are measured as multiples of $\hbar\omega_0$, time is measured in units of ω_0^{-1}, positions are measured as multiples of $[m\omega_0/\hbar]^{-1/2}$, momenta are measured in units of $[m\omega_0\hbar]^{1/2}$, where m ist the mass of the particle, ω_0 is the angular frequency of the basic oscillator, and $\hbar$ is Planck's constant divided by 2π.

  0005-9021/94/1212-1552 $ 10.00+.25/0

II. Newton's Equation of Motion

Since were are basically interested in the time evolution of given wave packets, the Schrödinger representation [2] is the most convenient one because in this representation all the time dependence is (for stationary Hamiltonians) focused on the wave functions.

Starting with a Hamiltonian

$$\hat{H} = \hat{H}_0 + V \tag{2.1}$$

where $\hat{H}_0$ is the Hamiltonian for which the eigenfunctions φ_k are known and V is a perturbation which doesn't necessarily have to be small.

Expanding the wave packet (the solution of the Schrödinger Eq. (1.1)) φ with respect to a set of basis functions formally gives

$$|\varphi\rangle = \sum_v c_v |\varphi_v\rangle \ . \tag{2.2}$$

We follow the arguments of Manz [3] and introduce formal position and momentum coordinates x_v and p_v respectively:

$$x_v = \mathrm{Re}(c_v) \ , \quad p_v = \mathrm{Im}(c_v) \ , \tag{2.3}$$

Multiplying Eqn. (1.1) from the left by $\langle\varphi_v|$ results in

$$\mathrm{i}(\dot{x}_u + \mathrm{i}\dot{p}_u) = \sum_v (x_v + \mathrm{i}p_v) H_{uv} \quad \text{with}$$
$$H_{uv} = \langle\varphi_u|\hat{H}|\varphi_v\rangle \ . \tag{2.4}$$

For bound systems the set of base functions can be chosen as a set of real functions which leads to a real symmetric matrix $H_{uv} = H_{vu}$.

From the real and imaginary part of Eqn. (2.4) it transpires that

$$\frac{\partial x_u}{\partial t} = \sum_v p_v H_{uv} \tag{2.5}$$

and

$$\frac{\partial p_u}{\partial t} = -\sum_v x_v H_{uv} \ . \tag{2.6}$$

We define a formal Hamiltonian as

$$H = \frac{1}{2} \sum_{u,v} (x_u x_v + p_u p_v) H_{uv} \tag{2.7}$$

and see that

$$\frac{\partial H}{\partial x_u} = \sum_v x_v H_{uv} \tag{2.8}$$

and

$$\frac{\partial H}{\partial p_u} = \sum_v p_v H_{uv} \ . \tag{2.9}$$

Consequently

$$\frac{\partial x_u}{\partial t} = \frac{\partial H}{\partial p_u} \ , \quad \frac{\partial p_u}{\partial t} = -\frac{\partial H}{\partial x_u} \ , \tag{2.10}$$

which are the Hamilton-Jacobi equations of motion for a classical oscillator in n dimensions (where n is the dimension of the basis set) [3] with the momentum and position components p_v and x_v, i.e. we have reduced the approximate solution of the time dependent Schrödinger Eq. (1.1) to a problem which can be treated with methods used in Newtonian dynamics.

It should be noted here that Eq. (2.10) is also valid when the physical problem under consideration is not stationary, i.e. if the Hamiltonian H is explicitly time dependent. However, one cannot say anything about the stability of the solution without first considering the explicit form of the perturbation.

For time independent Hamiltonians the dynamics of the whole system is linear, i.e. all n-dimensional trajectories are expected to be stable. For this latter case one can take the conservation of the energy as a criterion for the stability of the numerical procedure.

Since the numerical integration of the classical motion (for example in most molecular dynamics algorithms like the Verlet scheme [4]) in most cases does not start from Hamilton-Jacobi type equations of motion but from Newton's equation of motion, it is also reasonable to use this type of numerical integration scheme for the quantum motion. A transformation to Newton's type of equation is easily possible for the formalism based on the Schrödinger representation (see section 2.1); at least in those cases where the Hamiltonian is not explicitly time dependent. From Eqns. (2.5) and (2.6) one obtains Newton's equation of motion

$$\frac{\partial^2 x_u}{\partial t^2} = -\sum_v A_{uv} x_v \ , \quad \frac{\partial^2 p_u}{\partial t^2} = -\sum_v A_{uv} p_v \tag{2.11}$$

with

$$A_{uv} = \sum_t H_{ut} H_{tv} \tag{2.12}$$

which can be integrated with standard MD procedures for multi particle systems using, for example, the Verlet scheme [4].

III. Time Dependent SCF Formalism

Important formalisms available for approximate solutions of the time dependent Schrödinger Eq. (1.1) are time-dependent self-consistent field (TDSCF) methods [5 – 9]. The formalism of this type of approximation is presented

e in a form which is suitable for transformation to sets classical equations of motion.

In the TDSCF approximation we start with a Hamiltonian $\hat{H}$ which may be given in the form

$$= \sum_{i=1}^{k} \hat{h}_i(\hat{x}_i) + V(\hat{x}_1, \hat{x}_2, \ldots, \hat{x}_k) \tag{3.1}$$

here $\hat{x}_i$ represents sets of coordinates and corresponding omenta with pairwise empty intersections, i.e. the amiltonians $\hat{h}_i$ only depend on the set x_i, and V is a term oupling these sets. The solution of Eqn. (1.1) is then approximated by [6]

$$\varphi\rangle_t = \prod_{j=1}^{k} |n_j\rangle_t \exp(\mathrm{i}F_j(t)) = \prod_{j=1}^{k} |\bar{n}_j\rangle \tag{3.2}$$

where $|n_i\rangle$ are functions depending on the i-th coordinate et (in position representation) and on time. Setting Eqn. (3.2) into Eqn. (1.1) and multiplying from the left with

$$\prod_{j}^{(l)} \langle \bar{n}_j| = \prod_{j=1\, j\neq l}^{k} \langle \bar{n}_j| \tag{3.3}$$

results in

$$\mathrm{i}\frac{\partial}{\partial t}|\bar{n}_l\rangle = [\hat{h}_l^{\mathrm{SCF}} - G_l(t)]\,|\bar{n}_l\rangle \tag{3.4}$$

where $\hat{h}_l^{\mathrm{SCF}}$ is the SCF Hamiltonian for the l-th set

$$\hat{h}_l^{\mathrm{SCF}} = \hat{h}_l + \prod_{j}^{(l)} \langle n_j | V \prod_{i}^{(l)} |n_i\rangle \ . \tag{3.5}$$

$G_l(t)$ is a real function (see appendix A)

$$G_l(t) = \sum_{j}^{(l)} \left[\mathrm{i}\langle \bar{n}_j | \frac{\partial \bar{n}_j}{\partial t}\rangle - \langle \bar{n}_j | \hat{h}_j | \bar{n}_j\rangle \right] \tag{3.6}$$

determining the phase factors $F_l(t)$ in Eq. (3.2)

$$F_l(t) = \int_0^t G_l(\tau)\,\mathrm{d}\tau \ . \tag{3.7}$$

From Eqs. (3.4) to (3.7) the TDSCF equations for the individual components become

$$\mathrm{i}\frac{\partial}{\partial t}|\bar{n}_l\rangle = \hat{h}_l^{\mathrm{SCF}}\,|n_l\rangle \ . \tag{3.8}$$

The explicit determination of the phase factors is not simple since the integrant G_l in Eq. (3.7) depends on the phase factors $F_j(t)$ with j not equal to 1. Fortunately the phase factors are irrelevant as long as only expectation values with respect to the TDSCF functions (Eqn. (3.2)) are calculated, as it is done in this paper.

IV. Classical Equations of Motion

4.1 The "Exact" Solution

In the following section, we restrict the formalism to problems where only two set of coordinates are considered, i.e. where the Hamiltonian Eqn. (3.1) takes the form

$$\hat{H} = \hat{h}_x(\hat{x}) + \hat{h}_y(\hat{y}) + V(\hat{x}, \hat{y}) \ . \tag{4.1}$$

The generalisation of the formalism to more than two sets is straightforward. The eigenstates of $\hat{H}$ can then be approximated as linear combinations of product states ($|u_i\rangle|v_j\rangle$) where $|u_i\rangle$ and $|v_j\rangle$ are eigenstates of the zero order Hamiltonians $\hat{h}_x$ and $\hat{h}_y$, respectively:

$$|\varphi\rangle = \sum_{i=1}^{N_x}\sum_{j=1}^{N_y} c_{ij}\,|u_i\rangle|v_j\rangle \equiv \sum_{ij} c_{ij}\,|u_i\rangle|v_j\rangle \tag{4.2}$$

with

$$\hat{h}_x|u_i\rangle = \varepsilon_i^x|u_i\rangle \ , \quad \hat{h}_y|y_j\rangle = \varepsilon_j^y|v_j\rangle \ . \tag{4.3}$$

The set of basis functions is not necessarily a tensor product base, i.e. the pairs ($|u_i\rangle, |v_j\rangle$) may be chosen according to an energy condition such as

$$\varepsilon_i^x + \varepsilon_j^y \leq E_{\max} \ . \tag{4.4}$$

Setting

$$x_{ij} = \mathrm{Re}\,(c_{ij}) \ , \quad p_{ij} = \mathrm{Im}\,(c_{ij}) \tag{4.5}$$

Newton's equations of motion (Eqs. (2.11) and (2.12)) read

$$\frac{\partial^2 x_{ij}}{\partial t^2} = -\sum_{mn}\left(\sum_{kl} H_{ij,kl}H_{kl,mn}\right)x_{mn} \tag{4.6a}$$

$$\frac{\partial^2 p_{ij}}{\partial t^2} = -\sum_{mn}\left(\sum_{kl} H_{ij,kl}H_{kl,mn}\right)p_{mn} \tag{4.6b}$$

with the matrix elements

$$H_{ij,mn} = (\varepsilon_i^x + \varepsilon_j^y)\delta_{im}\delta_{jn} + \langle v_j|\langle u_i|V|u_m\rangle|v_n\rangle \tag{4.7}$$

where δ_{ik} is the Kronecker symbol.

4.2 The TDSCF Solution

Following the argument outlined in section III the time dependent solution of the dynamic Eq. (1.1) is approximated within the TDSCF scheme

$$|\varphi\rangle_t = |\varphi_x\rangle_t|\varphi_y\rangle_t \tag{4.8}$$

where now the individual states become

$$|\varphi_x\rangle = \sum_{i=1}^{N_x} c_i^x|u_i\rangle \ , \quad |\varphi_y\rangle = \sum_{j=1}^{N_y} c_j^y|v_j\rangle \tag{4.9}$$

ading to the SCF-Hamiltonians

$$\overset{\text{SCF}}{x} = \hat{h}_x + \sum_{im} c_i^{y*} c_m^y V_{im}^y(\hat{x}) \ ,$$

$$\overset{\text{SCF}}{y} = \hat{h}_y + \sum_{jn} c_j^{x*} c_n^x V_{jn}^x(\hat{y}) \tag{4.10}$$

ith

$$V_{im}^y = \langle v_i | V | v_m \rangle \ , \quad V_{jn}^x = \langle u_j | V | u_n \rangle \ . \tag{4.11}$$

he introduction of generalized coordinates and momenta

$$Q_i^x = \mathrm{Re}\,(c_i^x) \ , \quad P_i^x = \mathrm{Im}\,(c_i^x) \ ,$$
$$Q_j^y = \mathrm{Re}\,(c_j^y) \ , \quad P_j^y = \mathrm{Im}\,(c_j^y) \tag{4.12}$$

eads to the "classical" equations of motion (see Eqs. (2.8) and (2.9) in paper I)

$$\frac{\partial Q_i^x}{\partial t} = \sum_m [P_m^x A_{im} + Q_m^x B_{im}] \ ,$$

$$\frac{\partial P_i^x}{\partial t} = -\sum_m [Q_m^x A_{im} - P_m^x B_{im}] \tag{4.13}$$

with

$$A_{im} = \varepsilon_i^x \delta_{im} + \sum_{jn} [Q_j^y Q_n^y + P_j^y P_n^y] V_{ij,mn} \ ,$$

$$B_{im} = \sum_{jn} [Q_j^y P_n^y - P_j^y Q_n^y] V_{ij,mn} \tag{4.14}$$

and the matrix elements of the coupling term defined in Eq. (4.7). The equations of motion for Q_j^y and P_j^y are symmetrical to Eqs. (4.13) and (4.14). The coupling term V leads to a system of $N_{\text{SCF}} = N_x + N_y$ non-linearly coupled equations of motion in contrast to $N = N_x \cdot N_y$ linear equations in the "exact" solution with a tensor product basis set.

The stability of a numerical procedure for solving these equations can be tested in both cases considering that the norm and the energy of the system are stationary [6].

V. Wave Packet Dynamics in Two Dimensions

5.1 Model System

The formalism described above has been applied to a two-dimensional vibrational system with strong anharmonicities and a strong, non-linear coupling term

$$\hat{H} = \hat{h}_x + \hat{h}_y + 0.1\,\hat{x}^2\hat{y}^2 \tag{5.1}$$

with the zero order Hamiltonians

$$\hat{h}_x = \frac{1}{2}\left[-\frac{\partial^2}{\partial x^2} + \hat{x}^2\right] - 0.05\,\hat{x}^3 + 0.00140625\,\hat{x}^4 \tag{5.2}$$

and

$$\hat{h}_y = \frac{1}{2}\left[-\frac{\partial^2}{\partial y^2} + 1.44\,\hat{y}^2\right] - 0.0864\,\hat{y}^3 + 0.002916\,\hat{y}^4 \ . \tag{5.3}$$

This model system has already been studied classically and quantum mechanically by two of the authors [9, 10]. Classically, this system displays chaotic behavior even at very low energies [10] but it has been demonstrated that the quantum spectrum is much more regular than one should expect from the classical results. Even for quantum numbers $n > 100$ there are eigenstates with a clear nodal structure.

5.2 Initial Conditions and Dynamical Quantities

In this study we used minimum uncertainty Gaussian wave packets (harmonic oscillators coherent states, HOCSs) as initial states. The expectation values $\langle x \rangle$ and $\langle p \rangle$ of the position and the momentum, respectively, follow the classical equations of motion in the one-dimensional harmonic oscillator while the amplitude remains Gaussian. The analytic properties of HOCSs [11 – 17] and the special form of the potential, presented as a power series in the x- and y-direction with coupling term $0.1\,\hat{x}^2\hat{y}^2$, enable us to determine the energy expectation values of HOCSs analytically after normal ordering of the total Hamiltonian $\hat{H}$ [see appendix B]. As an initial state, we have chosen two harmonic oscillator coherent states $|\alpha\beta\rangle_a$ and $|\alpha\beta\rangle_b$, located at

a) $x^a(0) = 0.2931$, $y^a(0) = 1.8069$, $p_x^a(0) = -0.5724$,
$p_y^a(0) = 0.12828$ with ${}_a\langle\alpha\beta|\hat{H}|\alpha\beta\rangle_a = 3.2164$

and

b) $x^b(0) = 5.6100$, $y^b(0) = -0.0851$, $p_x^b(0) = 0.3368$,
$p_y^b(0) = 1.6134$ with ${}_b\langle\alpha\beta|\hat{H}|\alpha\beta\rangle_b = 11.8443$,

The dynamics of the two-dimensional wave packets is analyzed by considering the non-decay probability function [11]

$$P_{\alpha\beta}(t) = |\langle\alpha\beta(0)\,|\,\alpha\beta(t)\rangle|^2 \ , \tag{5.4}$$

the energy of the individual modes

$$E_x(t) = \langle\alpha\beta(t)\,|\,\hat{h}_x(\hat{x})\,|\,\alpha\beta(t)\rangle \ ,$$
$$E_y(t) = \langle\alpha\beta(t)\,|\,\hat{h}_y(\hat{y})\,|\,\alpha\beta(t)\rangle \ , \tag{5.5}$$

and the coupling energy

$$E_c(t) = \langle\alpha\beta(t)\,|\,0.1\,\hat{x}^2\hat{y}^2\,|\,\alpha\beta(t)\rangle \tag{5.6}$$

for both the "exact" solution (calculated within the traditional variational scheme) and the TDSCF approximation.

Within the variational scheme [10], we have calculated the eigenstates and energies of the total two-dimensional

Hamiltonian, (Eq. (4.1)), in the basis of the product eigenstates of the two zero order Hamiltonians (Eqs. (4.2) and (4.3)). Then, the time evolution of the initial HOCSs can be expanded in a basis of n eigenstates $|\phi_i\rangle$ of the total Hamiltonian [see Eq. (C9) in appendix C]. As in paper I, the size n of the basis ($|\phi_i\rangle, i = 1, n$) was chosen by considering the expansion coefficient $D_n = \langle\phi_n|\alpha\beta\rangle$ of the initial wave packet with respect to the eigenstate $|\phi_n\rangle$ of the total Hamiltonian, in such a way that the coefficient with the highest quantum number did not exceed a value of 10^{-5}.

Within the TDSCF scheme [see appendix D], the expansion coefficients Eqn. (4.9) of the wave packet have been calculated numerically by a Runge-Kutta integration of a set of Hamilton-Jacobi Eq. of motion (4.13) with different time increments Δt: $10^{-4} \leq \Delta t \leq 3 \cdot 10^{-3}$.

The deviation

$$\delta(t) = 1 - P^{\text{EXACT,TDSCF}}(t) \tag{5.7}$$

between the "exact" and the TDSCF solution [see appendix E] has been defined by evaluating the square of the overlap

$$P^{\text{EXACT,TDSCF}}(t) = |{}^{\text{EXACT}}\langle\alpha\beta(t)|\alpha\beta(t)\rangle^{\text{TDSCF}}|^2 , \tag{5.8}$$

which has to be unity at $t = 0$.

5.3 Numerical Results

The propagation of two wave packets (low and high energy) have been analyzed for both dynamical treatments in terms of single-mode energy expectation values and coupling terms as a function of time, and FFT characteristics of non-decay probability functions. The deviation $\delta(t)$ has been calculated to compare TDSCF results with the numerically "exact" solutions for the dynamics of wave packets in the model system.

We have considered the behavior of a wave packet $|\alpha\beta\rangle_a$ with a mean energy $\langle E\rangle = 3.2164$. This has been located in the harmonic regime (where the potential function can be approximated by a quadratic potential). Fig. 1a shows the time series of the energies $E_x(t)$, $E_y(t)$, the coupling term $E_c(t)$ and the total energy $E_{\text{tot}}(t)$ with a time increment 0.1 for 1024 time steps calculated by the variational method. Therefor, 60 harmonic oscillator eigenstates have been used for the calculation of the one-dimensional anharmonic eigenstates and the energies of the zero order Hamiltonians $\hat{h}_x(\hat{x})$ and $\hat{h}_y(\hat{y})$. The eigenstates and energies of the total Hamiltonian have been computed with a basis size of $n = 300$ product eigenstates of the two zero order Hamiltonians. The total energy $E_{\text{tot}}(t)$ varies within an absolute error of $\Delta E = 2 \cdot 10^{-3}$, whereas the error of the norm does not exceed a value of 10^{-5}.

It appears that most of the energy of the HOCS $|\alpha\beta\rangle_a$ is in the y-mode and the time series of the energies $E_x(t)$ and $E_y(t)$ are almost constant, close to that for two harmonic oscillators. With the same initial conditions, the time series of the energies $E_x(t)$, $E_y(t)$ and ($E_c(t)$ (see Fig. 1b) have

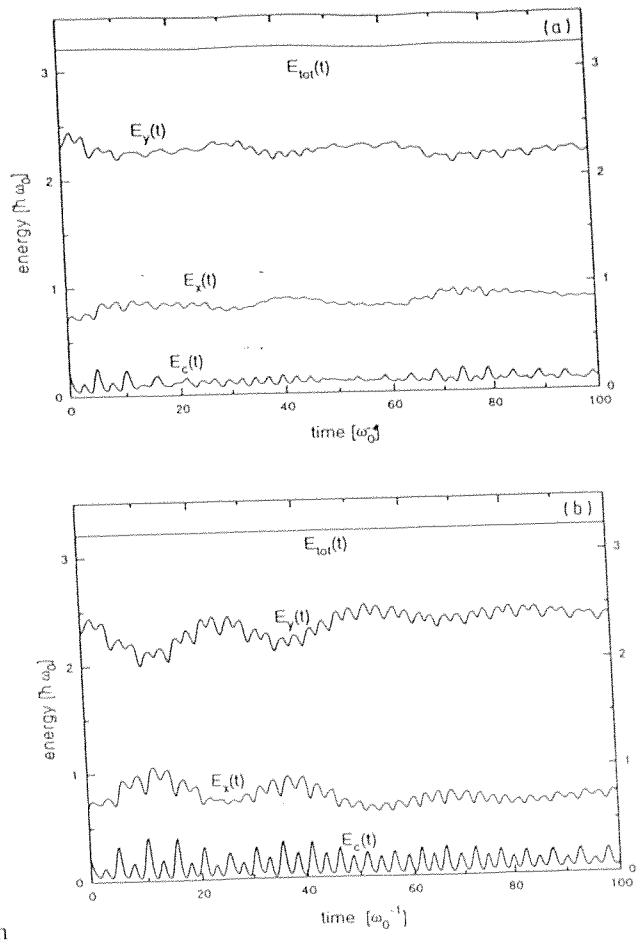

Fig. 1
Time evolution of the energy contents $E_x(t)$, $E_y(t)$ of the individual modes and the coupling energy $E_c(t)$ of an initial minimum uncertainty wave packet with mean energy $\langle E\rangle = 3.216$ (a) for the reference method and (b) within the TDSCF approximation

been calculated in the TDSCF approach, with a time increment 0.0025 for 40000 time steps (i.e. a total time of 100.0). The energy $E_{\text{tot}}(t)$ and the norm vary within an error of less than 0.01%. The TDSCF solutions in Fig. 1b and the "exact"-solutions in Fig. 1a agree fairly well for a very short time (several time units), but differ significantly for the remainder of the time interval. These differences between the "exact" and the TDSCF results are not due to technical reasons, as the use of smaller time increments or larger basis sets do not improve the numerical results. Fig. 1b shows that the TDSCF time series are predominantly periodic and have larger amplitudes than the corresponding "exact" time series in Fig. 1a. The results indicate that the quality of the TDSCF approximation deteriorates rapidly with time. An appropriate choice of coordinates [6b, 18] or the inclusion of additional configurations [19] may reduce the deviation of TDSCF expectation values from "exact" results as a function of time.

If the wave packet $|\alpha\beta\rangle$ is in the harmonic regime, Ehrenfest's theorem ensures that the average position and momentum of the wave packet is very close to the classical value at any time. Taking into consideration the necessary

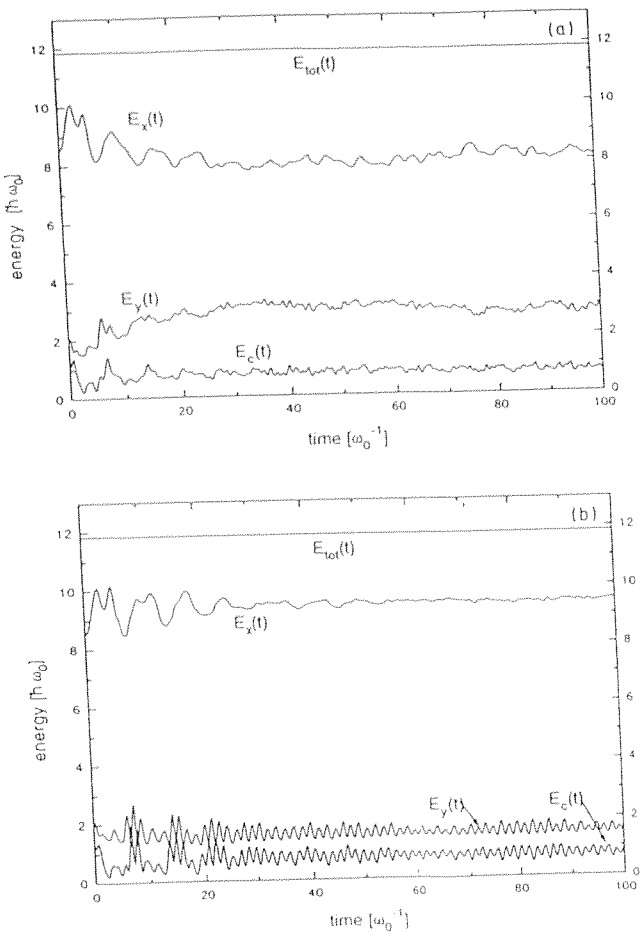

Fig. 2
Time evolution of the energies $E_x(t)$, $E_y(t)$ of a wave packet with mean energy $\langle E\rangle = 11.844$ (a) for the reference method and (b) within the TDSCF approximation

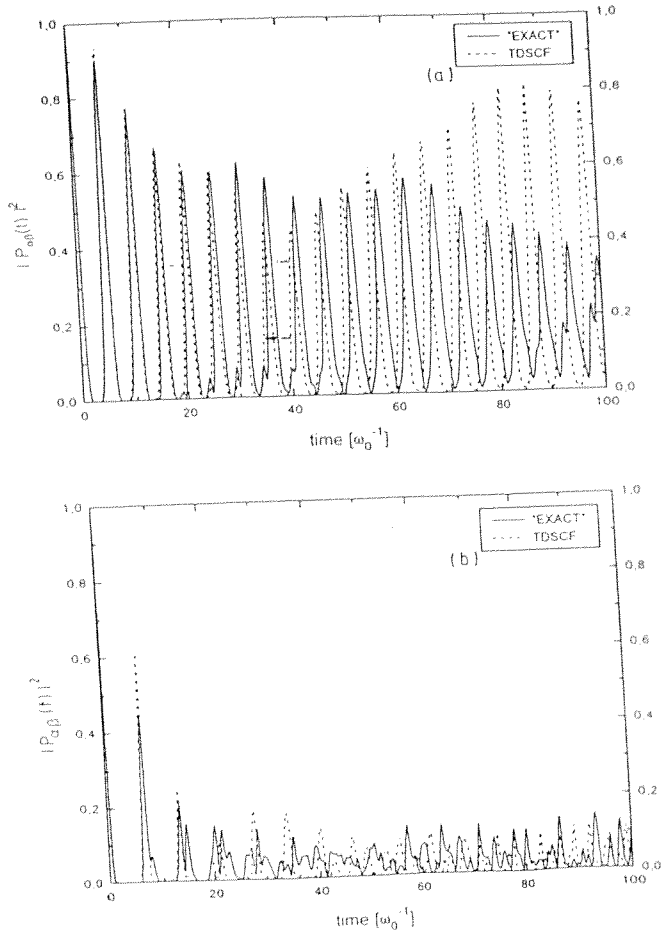

Fig. 3
Time series of the non-decay probability function $P_{\alpha\beta}^{\mathrm{EXACT}}(t)$ and $P_{\alpha\beta}^{\mathrm{TDSCF}}(t)$ of a wave packet (a) with mean energy $\langle E\rangle = 3.216$ and (b) with mean energy $\langle E\rangle = 11.844$

regular-classical-like dynamics of the center of the wave packet, one can expect large and periodic oscillations of the non-decay probability function, $P_{\alpha\beta}(t) = |\langle\alpha\beta(0)|\alpha\beta(t)\rangle|^2$ in both methods over a long period of time.

The quantities $P_{\alpha\beta}^{\mathrm{EXACT}}(t)$ and $P_{\alpha\beta}^{\mathrm{TDSCF}}(t)$ are plotted in Fig. 3a, confirming the arguments of the appearance of large periodic oscillations. The peak positions and heights qualitatively agree well for roughly 25 time units, but there are discrepancies for larger times t. It is evident that the "exact" state decays faster than the TDSCF solution. These discrepancies might result from the inadequate description of the energy transfer between the modes as a function of time in the TDSCF framework [6c].

We also have calculated the power spectral densities of the non-decay probability functions using fast Fourier transform (see Fig. 4). Both power spectral densities are mainly composed of two peaks at $\omega = 1.2 \pm 0.016$ and $\omega = 2.4 \pm 0.016$. The absolute error is half the frequency interval. Since in this example most of the energy of the initial wave packet $|\alpha\beta\rangle_a$ is localized in the y-mode (see Fig. 1a or 1b), peaks have to occur at the harmonic frequency $\omega_y = 1.2$ and at multiples of $\omega = 1.2$. One can see in the power spectrum of $P_{\alpha\beta}^{\mathrm{EXACT}}(t)$ that the peaks in Fig. 4a are smaller relative to those for the TDSCF method (Fig. 4b), because the time series for the reference method is less oscillatory.

In order to determine quantitatively the deviation between the "exact" and the TDSCF solution, we have calculated the quantity $\delta(t)$ [Eqn. (5.7), see also appendix E] with the same simulation parameters that have been used for the determination of the time series in Fig. 1a and 1b. In Fig. 6a, the aforementioned deviation starts with $\delta(t = 0) = 0$, since the expansion coefficients of the initial wave packet $|\alpha\beta\rangle_a$, for both dynamical treatments are the same. $\delta(t)$ is an increasing function of time and is larger than 0.9 after about 80 time units; i.e. after this time there is no correlation between the expansion coefficients of the TDSCF approximation and the coefficients of the numerically "exact" solution. Note that the quantities $P_{\alpha\beta}^{\mathrm{EXACT}}(t)$ and $P_{\alpha\beta}^{\mathrm{TDSCF}}(t)$ displayed in Fig. 3a agree fairly well for about the first 25 time units. At the time $t = 25$, the square of the overlap between $|\alpha\beta\rangle_a^{\mathrm{EXACT}}$ and $|\alpha\beta\rangle_a^{\mathrm{TDSCF}}$ is about 50%.

We also focus on the behavior of a wave packet $|\alpha\beta\rangle_b$ with a mean energy $\langle E\rangle = 11.8443$ that belongs to the anharmonic regime (close to the plateau value $E = 15$). The "ex-

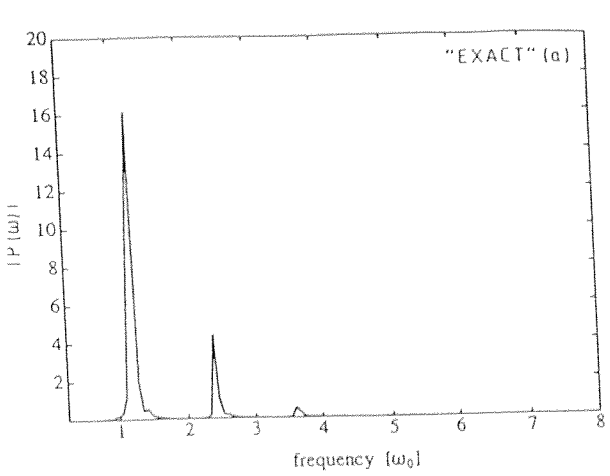

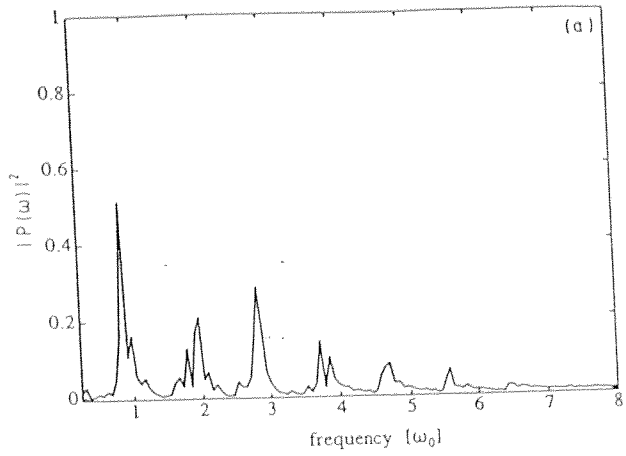

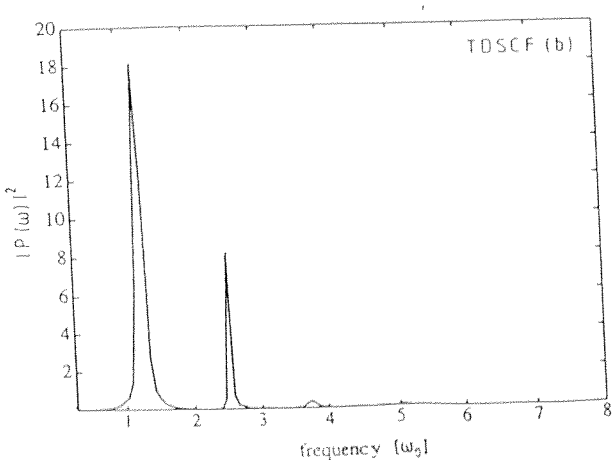

Fig. 4
Power spectral density, $|P(\omega)|^2$, of the non-decay probability function, $P_{\alpha\beta}(t)$, of a wave packet with mean energy $\langle E\rangle = 3.216$ (a) for the reference method and (b) within the TDSCF approximation

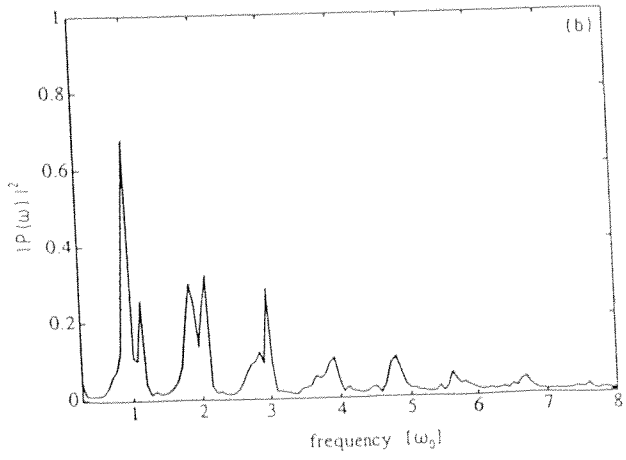

Fig. 5
Power spectral density, $|P(\omega)|^2$, of the non-decay probability function, $P_{\alpha\beta}(t)$, of a wave packet with mean energy $\langle E\rangle = 11.844$ (a) for the reference method and (b) within the TDSCF approximation

act" time series of the energies $E_x(t)$, $E_y(t)$ and $E_c(t)$ (see Fig. 2a) have been calculated using the same set of simulation parameters as for the lower energy with the exception of the choice of the basis set size n. The basis set size $n = 500$ assures that the variations of the total energy remains within an absolute error $\Delta E = 5 \cdot 10^{-3}$, whereas the error in the norm is again less than 10^{-5}.

Fig. 2a shows that most of the energy of the wave packet is located in the x-mode. It can be seen that one energy quantum is transferred from the x- to the y-mode during the time evolution, whereas the noisy coupling energy $E_c(t)$ fluctuates around one energy unit for the entire time interval. The time evolution of the individual energies $E_x(t)$, $E_y(t)$, $E_c(t)$ and the total energy $E_{\text{tot}}(t)$ of the wave packet $|\alpha\beta\rangle_b$ within the TDSCF approximation, is shown in Fig. 2b. In this case the time increment Δt is equal to 0.0025 and the total number of points for each time series is 1024. The time series of the energies $E_y(t)$ and $E_c(t)$ are almost periodic with a predominant frequency $\omega = 4.0$, which is a multiple of the harmonic frequency with respect to the x-coordinate. The transfer of an energy quantum from the high energy x-mode to the low energy y-mode can not be observed in Fig. 2a, confirming the arguments that TDSCF tends to produce too little energy transfer between the modes [6c].

The non-decay probability functions $P_{\alpha\beta}^{\text{EXACT}}(t)$ and $P_{\alpha\beta}^{\text{TDSCF}}(t)$ are displayed in Fig. 3b. They agree well during the time of their first fall-off (about seven time units). We expect many significant frequency components to appear in the Fourier expansion of these time series, since in this case the wave packet belongs to the anharmonic regime. This is confirmed in Fig. 5, which shows the power spectral densities of $P_{\alpha\beta}^{\text{EXACT}}(t)$ and $P_{\alpha\beta}^{\text{TDSCF}}(t)$. Examining the spectrum in Fig. 5a we see four peaks occuring at $\omega_1 = 0.88 \pm 0.016$, $\omega_2 = 1.89 \pm 0.016$, $\omega_3 = 2.89 \pm 0.016$ and $\omega_4 = 3.87 \pm 0.016$. These peaks can be identified as multiples of the harmonic frequency $\omega_x = 1.0$, shifted to lower frequencies by $\Delta\omega = 0.12$. In Fig. 5b, the power spectrum of $P_{\alpha\beta}^{\text{TDSCF}}(t)$ exhibits peaks at the frequencies $\omega_x = 1.0$ and $\omega_y = 1.2$ as well as some peaks at their linear combinations shifted to lower frequencies by $\Delta\omega = 0.06$.

The deviation $\delta(t)$ displayed in Fig. 6b has been calculated with the same simulation parameters that have been used for the determination of the time series in Fig. 2a

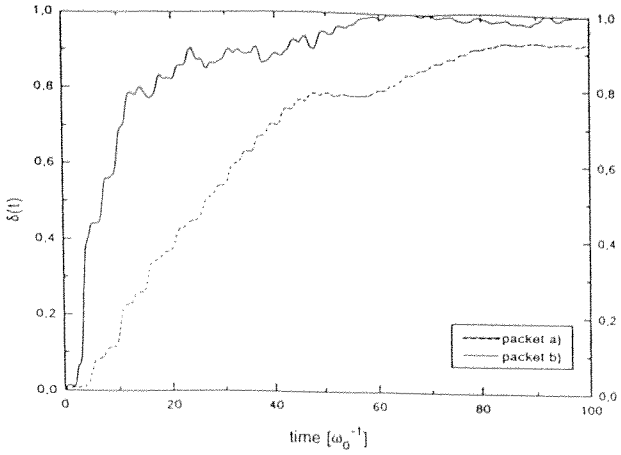

Fig. 6
Deviation between the reference and the TDSCF solution, $\delta(t)$, of a wave packet (a) with mean energy $\langle E\rangle = 3.216$ and (b) with mean energy $\langle E\rangle = 11.844$

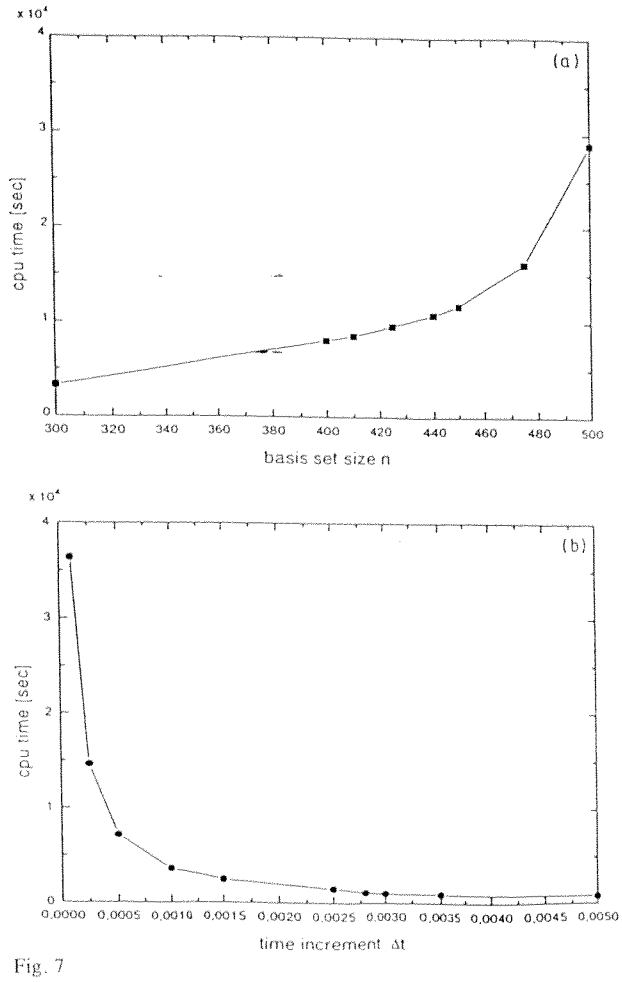

Fig. 7
(a) cpu time for 8 runs with different basis set sizes n (reference method) and (b) cpu time [s] versus different time steps (TDSCF approximation), after propagation of the wave packet with mean energy $\langle E\rangle = 11.844$ for 100 time units

and 2b. Fig. 6b shows that $\delta(t)$ is larger than 0.9 after about 50 time units. At time $t = 7$, the square of the overlap between $|\alpha\beta\rangle_a^{\text{EXACT}}$ and $|\alpha\beta\rangle_a^{\text{TDSCF}}$ is about 50%.

After propagation of the wave packet $|\alpha\beta\rangle_b$, with mean energy $\langle E\rangle = 11.844$ for 100 time units in the reference method, the cpu time is plotted as a function of eight different basis set sizes n in Fig. 7a. Fig. 7b shows the cpu time versus the time steps, after propagation of the packet $|\alpha\beta\rangle_b$ within the TDSCF approximation, for the same period of time as in Fig. 7a. For a fixed level of accuracy, e.g. for an error of less than 0.01% in the norm and energy, the time increment must be less than 0.0028. To obtain the results of the "exact" solution with the same level of accuracy the basis size n must be greater than 425.

From Fig. 7, the TDSCF scheme is roughly eight times as fast for the computation of the time dependent coefficients of the wave packet (and the required memory storage is much smaller) than the reference method.

VI. Conclusions

In this paper, we have made a comparison of the accuracy and efficiency of quantum mechanical wave packet propagation in a two-dimensional anharmonic system within the time dependent self-consistent field (TDSCF) approximation and a linear variational scheme as a reference method. The TDSCF formalism has been presented in a form which is suitable for the transformation to sets of classical equations of motion, as occurring in multiparticle classical dynamics; i.e. in the field of molecular dynamics, the TDSCF method is emerging as an important tool in the simulations of mixed classical-quantum systems.

Although the TDSCF method conserves the norm and energy, due to hermitian character of the TDSCF Hamiltonians, errors accumulate in the dynamic quantities of the wave packet. From the numerical calculations, we have found for the present model system and the selected initial conditions, the TDSCF results only agree well with reference results for a time scale of the first fall-off of the non-decay probability function. This is regardless of wether the wave packet is started in the low or high energy regime of the phase space.

The TDSCF method allows the flow of energy between the modes with the total energy remaining constant. Nevertheless, for a wave packet started in the anharmonic regime, the transfer of an energy quantum from the high energy x-mode to the low energy y-mode within the reference method cannot be observed in the corresponding plots for the TDSCF approximation. This confirms the arguments that TDSCF tends to underestimate the energy transfer between the modes.

The benchmark of the reference method and the TDSCF method assists in gaining an insight into the computational advantages of the TDSCF approximation technique. As a comparison between the TDSCF and the reference method for a given level of accuracy, e.g. of less than 0.01% error in energy and norm, computation of the time dependent coefficients of a wave packet in the TDSCF scheme is

roughly eight times as fast and the calculations require much less memory storage than the reference method.

Thus, we anticipate that future applications of the TDSCF approximation should be capable of handling mixed classical-quantum systems with many degrees of freedom.

This work has been supported by the Volkswagenstiftung, Hannover; TÜBITAK, Ankara (TBAG-1218); Minerva Gesellschaft für die Forschung mbH, Munich; German-Israeli Foundation for Scientific Research and Development (GIF).

Appendix A: G_l Functions

In order to demonstrate that the expressions $G_l(t)$ in Eq. (3.6) are real numbers, it is sufficient to demonstrate that all terms of the form $\langle n|\partial n/\partial t\rangle$ are imaginary. This can be easily demonstrated in the position space representation of the wave function $\varphi = \varphi(\tau, t)$ where τ is a coordinate set which may be correlated to one of the sets discussed above. Setting

$$\varphi = \varphi_R + i\varphi_I \ , \quad \varphi^* = \varphi_R - i\varphi_I \tag{A1}$$

one obtaines from the stationary of the normalisation integral

$$\frac{\partial}{\partial t}\int d\tau \varphi^* \varphi = 2\int d\tau \left(\frac{\partial \varphi_R}{\partial t}\varphi_R + \frac{\partial \varphi_I}{\partial t}\varphi_I\right) = 0 \tag{A2}$$

On the other hand one has

$$\int d\tau \varphi^* \frac{\partial \varphi}{\partial t} = \int d\tau \left(\varphi_R \frac{\partial \varphi_R}{\partial t} + \varphi_I \frac{\partial \varphi_I}{\partial t}\right) + i\int d\tau \left(\varphi_I \frac{\partial \varphi_R}{\partial t} - \varphi_R \frac{\partial \varphi_I}{\partial t}\right) \tag{A3}$$

i.e. this integral and so all terms of the type $\langle n|\partial n/\partial t\rangle$ are imaginary which proves that all $G_l(t)$ are real.

Appendix B: The Energy Expectation Values of Harmonic Oscillator Coherent States in a Two-Dimensional Anharmonic System

The coherent states $|\alpha\beta\rangle$ are product eigenstates of the annihilation operators $\hat{a}$, $\hat{b}$ with the eigenvalues α, β, respectively:

$$\hat{a}|\alpha\rangle = \alpha|\alpha\rangle \ , \quad \hat{b}|\beta\rangle = \beta|\beta\rangle \ . \tag{B1}$$

In Chap. V, we have chosen a model oscillator

$$\hat{H}(\hat{x},\hat{y}) = \hat{h}_x^0(\hat{x}) + \hat{h}_y^0(\hat{y}) + c_1\hat{x}^3 + c_2\hat{x}^4 + c_3\hat{y}^3 + c_4\hat{y}^4 + c_5\hat{x}^2\hat{y}^2 \ ,$$

with harmonic zero order Hamiltonians $\hat{h}_x^0(\hat{x})$ and $\hat{h}_y^0(\hat{y})$.

To calculate the energy expectation values of HOCSs analytically, we use the normal ordering formalism with the Boson creation and annihilation operators $\hat{a}^+$, $\hat{a}$ (for x-direction) and $\hat{b}^+$, $\hat{b}$ (for y-direction) to rewrite the Hamiltonian:

$$\hat{H}(\hat{a}^+, \hat{a}; \hat{b}^+, \hat{b}) = \sum_{pq} c_{pq}(\hat{a}^+)^p \hat{a}^q + \sum_{mn} d_{mn}(\hat{b}^+)^m \hat{b}^n \ . \tag{B2}$$

The energy expectation value of the normal ordered operator function (B2) can be expressed by the corresponding classical value. For convenience, we will indicate an operator function of $\hat{a}^+$ ($\hat{b}^+$) and $\hat{a}$ ($\hat{b}$) by a bar if it is already in normal order.

The position operator of HOCSs along the x-component can formally be written in a normal ordered form as

$$\hat{\bar{x}} = \frac{1}{\sqrt{2\omega_x}}(\hat{a}^+ + \hat{a}) \ . \tag{B3}$$

With the commutator relation

$$[\hat{a}, \hat{a}^+] = \hat{a}\hat{a}^+ - \hat{a}^+\hat{a} = \hat{1} \ , \tag{B4}$$

one obtains

$$\hat{x}^2 = \frac{1}{2\omega_x}(\hat{a}^{+2} + 2\hat{a}^+\hat{a} + \hat{a}^2 + \hat{1}) = \overline{\hat{x}^2} + \frac{1}{2\omega_x} \ , \tag{B5}$$

$$\hat{x}^3 = \left(\frac{1}{2\omega_x}\right)^{3/2} \cdot (\hat{a}^+ + \hat{a})^3 = \overline{\hat{x}^3} + \frac{3}{2\omega_x}\bar{\hat{x}} \ , \tag{B6}$$

$$\hat{x}^4 = \left(\frac{1}{4\omega_x^2}\right) \cdot (\hat{a}^+ + \hat{a})^4 = \overline{\hat{x}^4} + \frac{3}{4\omega_x^2}(4\omega_x\overline{\hat{x}^2} + 1) \ . \tag{B7}$$

Eqns. (B5) – (B7) and the analogous equations for the y-component of the position operator lead to the following analytical form of the energy expectation value of HOCSs:

$$\begin{aligned}\langle\alpha\beta|\hat{H}|\alpha\beta\rangle = {} & \overline{\hat{h}_x^0} + \frac{\omega_x}{2} + \overline{\hat{h}_y^0} + \frac{\omega_y}{2} + c_1 \cdot \left(\overline{\hat{x}^3} + \frac{3}{2\omega_x}\bar{\hat{x}}\right) \\ & + c_2 \cdot \left(\overline{\hat{x}^4} + 3 \cdot \left(\frac{\overline{\hat{x}^2}}{\omega_x} + \frac{1}{4\omega_x^2}\right)\right) + c_3 \cdot \left(\overline{\hat{y}^3} + \frac{3}{2\omega_y}\bar{\hat{y}}\right) \\ & + c_4 \cdot \left(\overline{\hat{y}^4} + 3 \cdot \left(\frac{\overline{\hat{y}^2}}{\omega_y} + \frac{1}{4\omega_y^2}\right)\right) \\ & + c_5 \cdot \left(\frac{\overline{\hat{y}^2}}{2\omega_y} + \frac{\overline{\hat{y}^2}}{2\omega_x} + \frac{1}{4\omega_x\omega_y} + \overline{\hat{x}^2}\cdot\overline{\hat{y}^2}\right) \ .\end{aligned} \tag{B8}$$

Appendix C: The "Exact" Time Evolution of the Energies $E_x(t)$, $E_y(t)$, $E_e(t)$ and of the Non-Decay probability Function $P_{\alpha\beta}(t)$

The time evolution of a two-dimensional HOCS $|\alpha\beta(t)\rangle$ in a time independent system can formally be written as

$$|\alpha\beta(t)\rangle = e^{-i\hat{H}t}|\alpha\beta(0)\rangle \ , \tag{C1}$$

where the initial HOCS $|\alpha\beta(t)\rangle$ can be expanded in a basis of product eigenstates ($|k_x\rangle|k_y\rangle$) of two harmonic oscillators

$$|\alpha\beta(0)\rangle = \sum_{k_x k_y} d_{k_x} d_{k_y} |k_x\rangle|k_y\rangle \ , \tag{C2}$$

with the expansion coefficients

$$d_{k_x} = \frac{\alpha^{k_x}}{\sqrt{k_x!}} \cdot e^{-(|\alpha|^2/2)} \quad \text{and} \quad d_{k_y} = \frac{\beta^{k_y}}{\sqrt{k_y!}} \cdot e^{-(|\beta|^2/2)} \ . \tag{C3}$$

Also, the initial HOCS $|\alpha\beta(0)\rangle$ can be expanded in a basis of eigenstates of the total Hamiltonian with the eigenvalue equation

$$\hat{H}|\phi_\mu\rangle = E_\mu|\phi_\mu\rangle \ , \tag{C4}$$

with

$$|\phi_\mu\rangle = \sum_{kl} c_{kl}^\mu |u_k\rangle|v_l\rangle \ , \tag{C5}$$

id

$$\iota_k\rangle = \sum_{k_x} a^k_{k_x}|k_x\rangle\ , \quad |v_l\rangle = \sum_{k_y} b^l_{k_y}|k_y\rangle\ . \tag{C6}$$

)efining the expansion coefficients

$$)_\mu = \langle\phi_\mu|\alpha\beta\rangle = \sum_{kl} c^{\mu *}_{kl}\cdot\left(\sum_{k_x} d_{k_x}a^{k*}_{k_x}\right)\cdot\left(\sum_{k_y} d_{k_y}b^{l*}_{k_y}\right)\ , \tag{C7}$$

where $a^k_{k_x}$ ($b^l_{k_y}$) are expansion coefficients in a harmonic basis of the one-dimensional anharmonic eigenstates in x (y) direction with the corresponding eigenvalue equation

$$\hat{h}^{\text{anh}}_x|u_k\rangle = \varepsilon^x_k|u_k\rangle \quad (\hat{h}^{\text{anh}}_y|v_l\rangle = \varepsilon^y_l|v_l\rangle)\ . \tag{C8}$$

With the expansion coefficients D_μ of Eqn. (C7) and Eqn. (C5), one obtains the time evolution of HOCSs in a basis set of eigenstates of the total Hamiltonian

$$|\alpha\beta(t)\rangle = \sum_\mu D_\mu e^{-iE_\mu t}|\phi_\mu\rangle = \sum_{kl}(x_{kl}(t)+i\cdot p_{kl}(t))|u_k\rangle|v_l\rangle\ . \tag{C9}$$

Thus, the "exact" time evolution of the energy along the x-coordinate of HOCSs is:

$$\langle\alpha\beta(t)|\hat{h}_x(\hat{x})|\alpha\beta(t)\rangle = \sum_{kl}|x_{kl}(t)+i\cdot p_{kl}(t)|^2\cdot\varepsilon^x_k\ . \tag{C10}$$

The equations for the energy along the y-coordinate can be derived in an analogous way. The "exact" time evolution of the coupling term $E_c(t)$ can be written as

$$\langle\alpha\beta(t)|c_5\hat{x}^2\hat{y}^2|\alpha\beta(t)\rangle = c_5\sum_{ijkl}(x_{kl}(t)+ip_{kl}(t))(x_{ij}(t)-ip_{ij}(t))\cdot\langle u_i|\hat{x}^2|u_k\rangle\langle v_j|\hat{y}^2|v_l\rangle\ . \tag{C11}$$

The matrix elements in Eqn. (C11) are

$$\langle u_i|\hat{x}^2|u_k\rangle = \sum_m\langle u_i|\hat{x}|u_m\rangle\langle u_m|\hat{x}|u_k\rangle \tag{C12}$$

with

$$\langle u_i|\hat{x}|u_m\rangle = \sum_{k'_x k_x} a^{i*}_{k'_x}a^m_{k_x}\cdot\langle k'_x|\hat{x}|k_x\rangle\ , \tag{C13}$$

using the wellknown relation:

$$\hat{x}|k_x\rangle = \frac{1}{\sqrt{2\omega_x}}\left(\sqrt{k_x}|k_x-1\rangle+\sqrt{k_x+1}|k_x+1\rangle\right)\ . \tag{C14}$$

The non-decay probability function $P_{\alpha\beta}(t)$ of a time dependent wave packet is defined as

$$P_{\alpha\beta}(t) = |\langle\alpha\beta(0)|\alpha\beta(t)\rangle|^2\ . \tag{C15}$$

With Eq. (C9), the non-decay probability function becomes

$$P_{\alpha\beta}(t) = |\sum_{kl}(x_{kl}(0)-ip_{kl}(0))\cdot(x_{kl}(t)+ip_{kl}(t))|^2\ . \tag{C16}$$

Appendix D: The TDSCF Approximation of the Time Evolution of the Energies $E_x(t)$, $E_y(t)$, $E_c(t)$ and of the Non-Decay Probability Function $P_{\alpha\beta}(t)$

The coherent state $|\alpha\beta\rangle$ can be approximated as a linear combination of product states $|u_i\rangle|v_j\rangle$, where $|u_i\rangle|v_j\rangle$ are eigenstates of the one-dimensional, anharmonic Hamiltonians $\hat{h}^{\text{anh}}_x$ and $\hat{h}^{\text{anh}}_y$, respectively.

$$|\alpha\beta(t)\rangle = \sum_{ij} c^x_i(t)c^y_j(t)|u_i\rangle|v_j\rangle = |\alpha(t)\rangle|\beta(t)\rangle\ . \tag{D1}$$

The time evolution of the energy in x-direction (and similarly in y-direction) can be written as

$$\langle\alpha\beta(t)|\hat{h}_x|\alpha\beta(t)\rangle = \sum_{ijkl} c^{x*}_i(t)c^{y*}_j(t)c^y_l(t)\cdot\langle u_iv_j|\hat{h}_x|u_kv_l\rangle = \sum_i|c^x_i(t)|^2\cdot\varepsilon^x_i\ . \tag{D2}$$

The time evolution of the coupling term $E_c(t)$ within the TDSCF approximation can be calculated as

$$\langle\alpha\beta(t)|c_5\hat{x}^2\hat{y}^2|\alpha\beta(t)\rangle = c_5\langle\alpha(t)|\hat{x}^2|\alpha(t)\rangle\langle\beta(t)|\hat{y}^2|\beta(t)\rangle = c_5\sum_{ik}c^{x*}_i(t)c^x_k(t)\langle u_i|\hat{x}^2|u_k\rangle\cdot\sum_{jl}c^{y*}_j(t)c^y_l(t)\langle v_j|\hat{y}^2|v_l\rangle\ . \tag{D3}$$

In analogy to Eqs. (C12) – (C14) one obtains the matrixelements $\langle u_i|\hat{x}^2|u_k\rangle$. The non-decay probability function $P_{\alpha\beta}(t)$ is defined as

$$P_{\alpha\beta}(t) = |\langle\alpha\beta(0)|\alpha\beta(t)\rangle|^2\ . \tag{D4}$$

With Eq. (D1), $P_{\alpha\beta}(t)$ becomes

$$P_{\alpha\beta}(t) = |\sum_{kl}c^{x*}_k(0)\cdot c^{y*}_l(0)\cdot c^x_k(t)\cdot c^y_l(t)|^2\ . \tag{D5}$$

Appendix E: Deviation Between the "Exact" and the TDSCF Solution

The "exact" solution

$$|\alpha\beta(t)\rangle^{\text{EXACT}} = \sum_{kl}(x_{kl}(t)+ip_{kl}(t))|u_k\rangle|v_l\rangle\ . \tag{E1}$$

and the TDSCF solution

$$|\alpha\beta(t)\rangle^{\text{TDSCF}} = \sum_{ij}c^x_i(t)c^y_j(t)|u_i\rangle|v_j\rangle \tag{E2}$$

can be compared by considering the overlap between the "exact" wavepacket $|\alpha\beta(t)\rangle^{\text{EXACT}}$ and the approximated one $|\alpha\beta(t)\rangle^{\text{TDSCF}}$:

$$P^{\text{EXACT,TDSCF}}(t) = |{}^{\text{EXACT}}\langle\alpha\beta(t)|\alpha\beta(t)\rangle^{\text{TDSCF}}|^2 = |\sum_{kl}(x_{kl}(t)-ip_{kl}(t))\cdot c^x_k(t)c^y_l(t)|^2\ . \tag{E3}$$

We defined the quantity

$$\delta(t) = 1 - |^{\mathrm{EXACT}}\langle \alpha\beta(t) | \alpha\beta(t)\rangle^{\mathrm{TDSCF}}|^2 = 1 - P^{\mathrm{EXACT,TDSCF}}(t) \quad \text{(E4)}$$

to calculate the deviation between the "exact" and the TDSCF solution as a function of time.

References

[1] E. Yurtsever and J. Brickmann, Ber. Bunsenges. Phys. Chem. *98*, 554 (1994).

[2] A. Messiah, "Quantum Mechanics", Vol. 1, pp 310 – 323, North Holland Publ. Co., Amsterdam 1961.

[3] J. Manz, J. Chem. Phys. *91*, 2190 (1989).

[4] L. Verlet, Phys. Rev. *159*, 98 (1967).

[5] See for a review: R. Kosloff, J. Phys. Chem. *92*, 2087 (1988).

[6] (a) R.B. Gerber, V. Buch, and M.A. Ratner, J. Chem. Phys. *77*, 3022 (1982).
(b) R.B. Gerber and M.A. Ratner, Adv. Chem. Phys. *70*, 97 (1988).
(c) R. Alimi, R.B. Gerber, A.D. Hammerich, R. Kosloff, and M.A. Ratner, J. Chem. Phys. *93*, 6484 (1990).

[7] P. Hofmann and J. Brickmann, J. Chem. Phys. *88*, 6501 (1988).

[8] E. Yurtsever and T. Uzer, Ber. Bunsenges. Phys. Chem. *96*, 906 (1992).

[9] E. Yurtsever and J. Brickmann, Ber. Bunsenges. Phys. Chem. *96*, 142 (1992).

[10] E. Yurtsever and J. Brickmann, Ber. Bunsenges. Phys. Chem. *94*, 804 (1990).

[11] (a) J. Brickmann, J. Chem. Phys. *78*, 1984 (1982).
(b) J. Brickmann and P. Russegger, Chem. Phys. Lett. *89*, 239 (1982).
(c) J. Brickmann and P. Russegger, Chem. Phys. *68*, 369 (1982).

[12] For a review of wave packet dynamics see: E.J. Heller in "Chaos and Quantum Physics", pp 1 – 134, Nato Lectures, ed. by A. Voros, M. Gianonni, O. Bohigas. North Holland Publ. 1990.

[13] (a) R.L. Glauber, Phys. Rev. *130*, 2529 (1063); *131*, 2766 (1963), Phys. Lett. *21*, 650 (1966).
(b) E.H. Kerner, Can. J. Phys. *36*, 371 (1058).

[14] P. Caruther and M.M. Nieto, Am J. Phys. *33*, 537 (1965).

[15] (a) C.C. Gerry, Phys. Rev. *a33*, 2148 (1986).
(b) C.L. Mehta and E.C.G. Sudarshan, Phys. Lett. *23*, 574 (1966).

[16] R. Marquardt and M. Quack, J. Chem. Phys. *90*, 6320 (1989).

[17] J. Brickmann and P.C. Schmidt, Intern. J. Quantum Chem. *23*, 47 (1983).

[18] J. Kucar, H.D. Meyer, and L.S. Cederbaum, Chem. Phys. Lett. *140*, 525 (1987).

[19] A.D. Hammerich, R. Kosloff, and M.A. Ratner, Chem. Phys. Lett. *153*, 483 (1988).

(Received: July 8, 1994
final version: September 1, 1994)

E 8737

PHYSICAL REVIEW E VOLUME 50, NUMBER 5 NOVEMBER 1994

Quantal-classical mixed-mode dynamics and chaotic behavior

Ersin Yurtsever
Chemistry Department, Middle East Technical University, Ankara, Turkey
(Received 6 May 1994)

Dynamical behavior of a nonlinearly coupled oscillator system is studied under classical and quantal-classical mixed-mode conditions. Classically, the system displays chaos above an energy threshold. However, upon a partial quantization of the problem within a self-consistent-field formalism, the dynamics becomes highly periodic, pointing out to the smoothing process of the quantum mechanics.

PACS number(s): 05.45.+b, 03.65.Sq, 82.20.Rp

INTRODUCTION

Intramolecular vibrational relaxation and energy redistribution (IVR) have been among the most challenging problems of chemical physics [1]. The description of the internal motion of molecules, such that the energy in certain mode(s) is transferred to other modes, forms the subject of molecular dynamics and the mechanisms and time scales of these processes pose interesting questions. These phenomena are almost invariably modeled by nonlinear equations and there are different approaches of establishing dynamical equations and their solutions. The most simple and widely used methodology is the classical trajectory analysis in which the Newton, Lagrange, or Hamilton equations are solved for the nuclear motion along the Born-Oppenheimer potential energy surface. Once the hypersurface is obtained from quantum mechanical methods of various sophistication, or by fitting to the experimental data, numerical integration techniques can then be employed to follow the motion of atoms in the $6N$-dimensional phase space [2]. Despite its general success, this approach has some serious drawbacks. First of all, as the system gets larger, the proper sampling of the phase space gets more and more difficult; that is, the necessary number of trajectories for a detailed analysis becomes too large for practical purposes. But more importantly, classical analysis suffers from its inability to incorporate several quantum effects such as zero-point vibration and tunneling. Exclusion of these effects may result in even qualitatively incorrect descriptions of the system for certain cases. For example, a classical system may dissociate by the transfer of energy from one mode to the dissociating mode, whereas in quantum description of the system, the amount of energy transferred would be less due to the zero-point effect, and one may not observe any dissociation at all. On the other hand, a full quantum calculation of the dynamics of a reasonably large molecule is computationally very prohibitive. Even though fast Fourier transforms allow us to carry out such a task, at least for small systems [3,4], the computational burden is too heavy to analyze anything but small molecules. There is a third alternative to molecular dynamics in which both highly developed techniques of the classical algorithms are employed and some quantum effects are included. In the so-called mixed-mode molecular dynamics, classical and quantum approaches are used together [5–9]. The basis of such a mixed-mode approach lies in the fact that in large systems there is a great variety of frequencies, which can roughly be classified as hard and soft modes, so that the hard modes are treated quantum mechanically whereas the slower ones can be studied within classical mechanical approaches. Once this separation is achieved, time evolution equations can be solved in a self-consistent-field methodology [10–12]. This is analogous to the Born-Oppenheimer approximation, in which the fast electronic motion is solved with quantum mechanical methodology for the fixed nuclei since they move relatively slower compared to electrons. Subscribing to this point of view, an N-dimensional problem can be written as a sum of smaller dimensional problems in which nonlinear terms appear as time-dependent perturbations.

There is also another very strong motivation of a detailed description of the mixed-mode dynamics. The classical behavior of the Hamiltonian systems is generally well understood with all the measures such as Poincaré maps, Kolmogorov or information entropy, and Lyapunov exponents allowing one to determine the regular and chaotic regimes in the phase space [13,14]. However, the quantum dynamics suffer from the lack of such well-defined measures, which distinguish the regular and "irregular" behavior [15–17]. The previously suggested measures, such as statistical analysis of the eigenvalue spectra [18,19], sensitivity analysis [20–22], or autocorrelation functions [23], do not strictly respond the way the classical mechanical counterparts work. In fact, the field of "quantum chaology" now no longer searches for the quantum chaos, but rather tries to distinguish different qualitative behavior in the dynamics [24–27]. Mixed-mode methodology offers an intermediate step in which one can study purely classical measures of a system under the effect of a quantum field. We would like to refer to this mixing as "partial quantization," rather than the more general "semiclassical approach." The idea is that after partitioning the modes, classical ones can be studied in two parallel sets of computations. The first one is the fully classical one (FC) and the other one is the mixed-mode (MM). In both methods, one set of modes remains classical but they move under the effect of "similar" classical and quantum fields. Therefore, it is now possible to

1063-651X/94/50(5)/3422(9)/$06.00

: identical measures and observe changes upon uantization of the system.

MIXED-MODE DYNAMICS

ut loss of generality, let us begin with a two-onal oscillator system:

$$c,y)=H_x(x)+H_y(y)+V(x,y)\ , \tag{1}$$

$V(x,y)$ is a nonlinear coupling term, and it is as-hat there is no transformation to obtain a separ-m of the Hamiltonian. Within a self-consistent-CF) approximation we obtain two one-dimensional onians in the form of

$$^{CF}=H_x+\langle V(x,y)\rangle_y\ , \tag{2a}$$

$$^{CF}=H_y+\langle V(x,y)\rangle_x\ , \tag{2b}$$

$\langle\ \rangle$ denotes an appropriate average over the ng coordinate(s). Now the dynamical equations g these operators can be solved iteratively, that is, e evolution of the system along one coordinate is for a short time step under the influence of the : field of the other mode(s). Even though we do ve rigorous proof that the averaging process of uations does not destroy chaotic behavior, our ini-culations show that classical trajectories of such a do not show significantly different behavior than of the original Hamiltonian if the time step is ntly small, even under chaotic conditions.

: the new time-dependent SCF Hamiltonians are l (since average quantities are constant only for the on of the small time step, H_x^{SCF} and H_y^{SCF} are time lent), it is now possible to combine quantum and al dynamical equations with proper boundary con-. If we choose the x coordinate to be the classical to be the quantum coordinate, our initial system is l by a point in two-dimensional phase space (given and p_x) and a wave packet $\Psi(y,t)$ (for a better otion of the classical motion, an ensemble of initial nates can also be employed). In that case, dynami-uations become

$$_x/\partial t=-\partial H_x^{SCF}/\partial x\ , \tag{3a}$$

$$c/\partial t=\partial H_x^{SCF}/\partial p_x\ , \tag{3b}$$

$$i\partial\Psi(y,t)/\partial t=H_y^{SCF}\Psi(y,t)\ . \tag{3c}$$

sing λx^2y^2 as the nonlinear coupling, we now define Hamiltonians as

$$_x^{SCF}=H_x+\lambda\langle\Psi|y^2|\Psi\rangle x^2 \tag{4a}$$

$$_y^{SCF}=H_y+\lambda\{x^2\}y^2\ . \tag{4b}$$

$\langle\ \rangle$ is the quantum average of y^2 over the wave t and $\{\ \}$ is the square of the classical coordinate (again, for a bundle of trajectories, this is just an arithmetical average over all trajectories). The time evolution of classical trajectories can be obtained by the straighforward numerical integration techniques. The quantum equations can be solved by several methods. In order to carry out a systematic analysis, we decide to expand the initial wave packet as a linear combination of the eigenfunctions of the anharmonic oscillator H_y, and follow the time evolution again in terms of these basis functions. Our mixed mode system is chosen as [28,29]

$$\begin{aligned}H=&0.5(p_x^2+p_y^2+x^2+1.44y^2)-0.05x^3\\&+0.001\,406\,25x^4-0.0864y^3\\&+0.029\,16y^4+0.1x^2y^2\ .\end{aligned} \tag{5}$$

The coefficients of the polynomial are chosen such that there are no double minima, and inflection points along each coordinate are at the same level. This Hamiltonian does not have any symmetry and there is no degeneracy in either one-dimensional or two-dimensional eigenvalue spectra. The wave packet is written as

$$\Psi(y,t)=\sum b_p(t)\varphi_p(y)\ , \tag{6}$$

where $\varphi_p(y)$ is the eigenfunction of H_y with quantum number p.

$$H_y\varphi_p(y)=\varepsilon_p\varphi_p(y)\ . \tag{7}$$

Now the Schrödinger equation in atomic units can be written as

$$i\sum\dot{b}_p\varphi_p(y)=\sum b_pH_y\varphi_p(y)\ , \tag{8}$$

with $\dot{b}_p$ denoting the time derivative of expansion coefficients. By multiplying with φ_q from the left and integrating over the coordinate, we obtain

$$i\dot{b}_q=\sum b_pA_{qp}\ , \tag{9}$$

where the matrix A is defined through

$$A_{qp}=\delta_{qp}\varepsilon_p+\lambda\{x^2\}\int\varphi_p(y)y^2\varphi_p(y)dy\ . \tag{10}$$

In matrix notation, we obtain

$$i\dot{B}=AB\ . \tag{11}$$

The above equation can then be simply solved by,

$$iB=ACC^{-1}B\ . \tag{12}$$

Then,

$$iC^{-1}\dot{B}=C^{-1}ACC^{-1}B\ . \tag{13}$$

Defining $D=C^{-1}B$, we realize now a decoupled matrix equation,

$$i\dot{D}=ED\ , \tag{14}$$

where C is the pseudo-time-dependent unitary matrix that diagonalizes the Hermitian matrix A, E being a diagonal matrix with eigenvalues E_p. The solution is given as

$$_p = N_p^0 \exp(-iE_p t) , \quad (15)$$

N_p^0 being undetermined integration constants. ing in mind that the wave function must be continu- a time, that is,

$$\Psi^k(y,\delta t) = \Psi^{k+1}(y,0) , \quad (16)$$

d $(k+1)$ define here two successive time steps. The dary conditions can be expressed as

$$b_p^k(\delta t) = b_p^{k+1}(0) . \quad (17)$$

the final coefficients are

$$b_p^k(\delta t) = \sum C_{pm} d_m^{k+1}(0) , \quad (18)$$

$$d_m^{k+1}(0) = N_m^0 . \quad (19)$$

lly, we obtain formulas for time-dependent icients of the wave packet

$$B^k = C^{k+1} N^{k+1} \text{ and } N^{k+1} = B^k (C^{k+1})^{-1} . \quad (20)$$

RESULTS AND DISCUSSION

the Introduction, it is discussed that mixed-mode amics offers an extremely useful tool for the analysis ne irregular dynamics as we go along from the classi- to the quantum world. By quantizing part of the niltonian, one can still concentrate on the classical of the system, that is, deterministic properties such oordinates and momenta are analyzed instead of fol- ing the time evolution of average quantities of the ntum picture, which may give a completely different cription due to the smoothing processes. Since nitions of classical measures like Poincaré maps or apunov exponents of a mixed-mode system are some- at ambiguous, we proceed to compute the usual quan- s such as trajectories, time autocorrelation functions, Fourier transforms of several observables of "simi- " systems under fully classical (FC) and mixed-mode M) conditions. These conditions are defined as fol- s: for FC conditions, classical trajectories in the r-dimensional phase space are employed and for MM

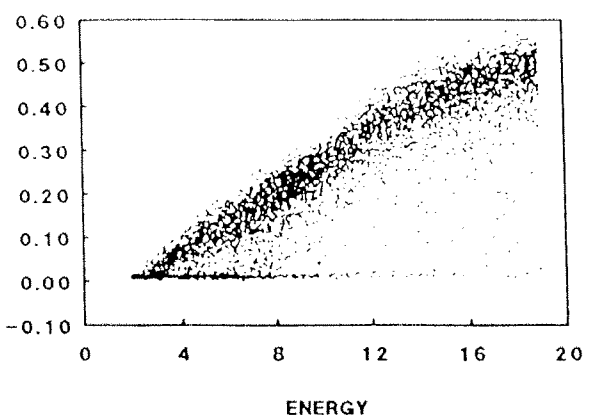

FIG. 1. Maximum Lyapunov exponents of the classical sys- n.

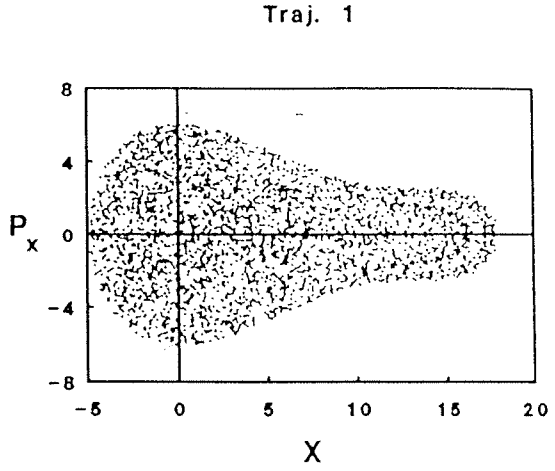

FIG. 2. Poincaré map of trajectory no. 1.

conditions, a combination of a classical trajectory in two-dimensions and a wave packet along the other coordinate forms the total system. In the model system, the x mode remains classical for both methodologies and the y mode is a quantal one for MM computations.

To summarize the classical behavior of this two-dimensional oscillator system, we present the Lyapunov exponent spectrum from 5500 trajectories as functions of the trajectory energy (Fig. 1). Lyapunov exponents are computed by the tangent space method [30,31], and the sum of all exponents remains less than 10^{-10} within our integration times of 500 units (10^5 steps). Throughout the discussion, generalized atomic units are employed and Lyapunov exponents are given in units of bits/time. Four-point constant-step Runge-Kutta integration is used to solve both nonlinear and linear equations. Lyapunov exponents generally converge around 250 units of time. At very low energies (there is only a single eigenvalue below 2.0 and 6 eigenvalues below 4.0), we start detecting positive Lyapunov exponents. The critical energy is around 8.0, after which there remains only a very small number of zero Lyapunov exponents. This small number of trajectories is attributed to initial conditions that are stuck in the deep valleys of the potential surface and can-

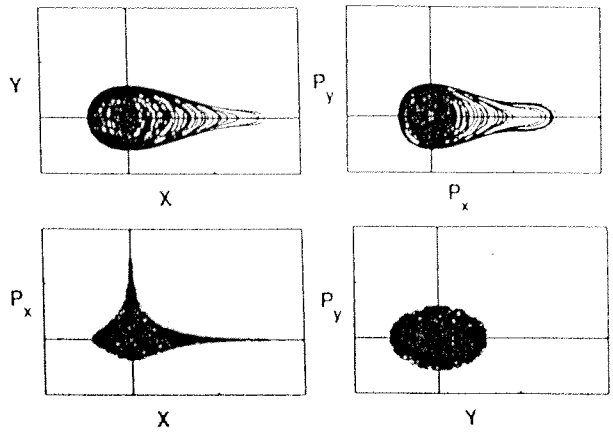

FIG. 3. Trajectory no. 1 along various cross sections of the phase space.

TABLE I. Initial conditions for classical trajectories.

Trajectory	y	P_y	E_y	E_c
1	1.943 652	1.655 468	3.497 499	0.023 611
2	−1.943 652	0.450 488	3.497 499	0.023 611
3	1.625 556	1.976 260	3.687 844	0.016 515
4	2.598 642	0.0	3.478 904	0.042 206

not escape within time scales of our numerical experiments. We conclude that the complete phase space is chaotic above this critical energy, and to fully realize the effects of quantization an energy value that lays in the completely chaotic regime is chosen for the comparison.

For the definition of the initial conditions for MM calculations, the coordinate and momentum along the x

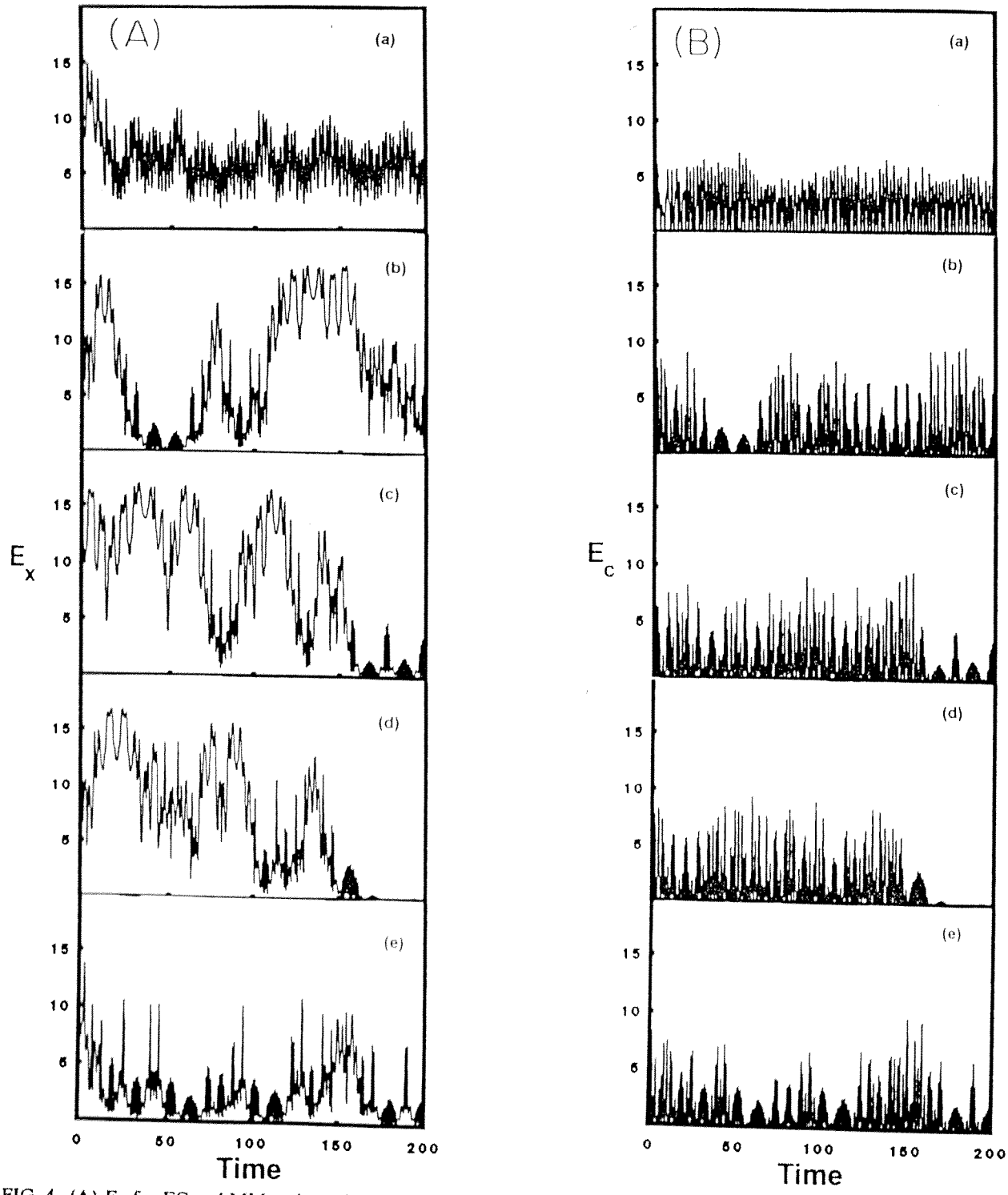

FIG. 4. (A) E_x for FC and MM trajectories. (a) Mixed mode, (b) trajectory no. 1, (c) trajectory no. 2, (d) trajectory no. 3, (e) trajectory no. 4. (B) E_c for FC and MM trajectories. (a) Mixed mode, (b) trajectory no. 1, (c) trajectory no. 2, (d) trajectory no. 3, (e) trajectory no. 4.

mode are chosen as $x=0.25$ and $p_x=5.471\,658\,94$, so that the classical energy is equal to 15.0. (Mode energies are computed only from Hamiltonians H_x or H_y, that is, the energy in the coupling is excluded.) Along the y mode, a wave packet as an equally weighed linear combination of the anharmonic oscillator eigenfunctions with quantum numbers 2 and 3 is used.

$$\Psi(y,0)=(1/\sqrt{2})(\varphi_2+\varphi_3)\,. \tag{21}$$

The quantum energy is then equal to 3.497 498 97, coupling energy is 0.023 611 15, and the total energy is 18.521 110 12.

The selection of the classical counterpart of the initial conditions for FC computations poses a severe problem;

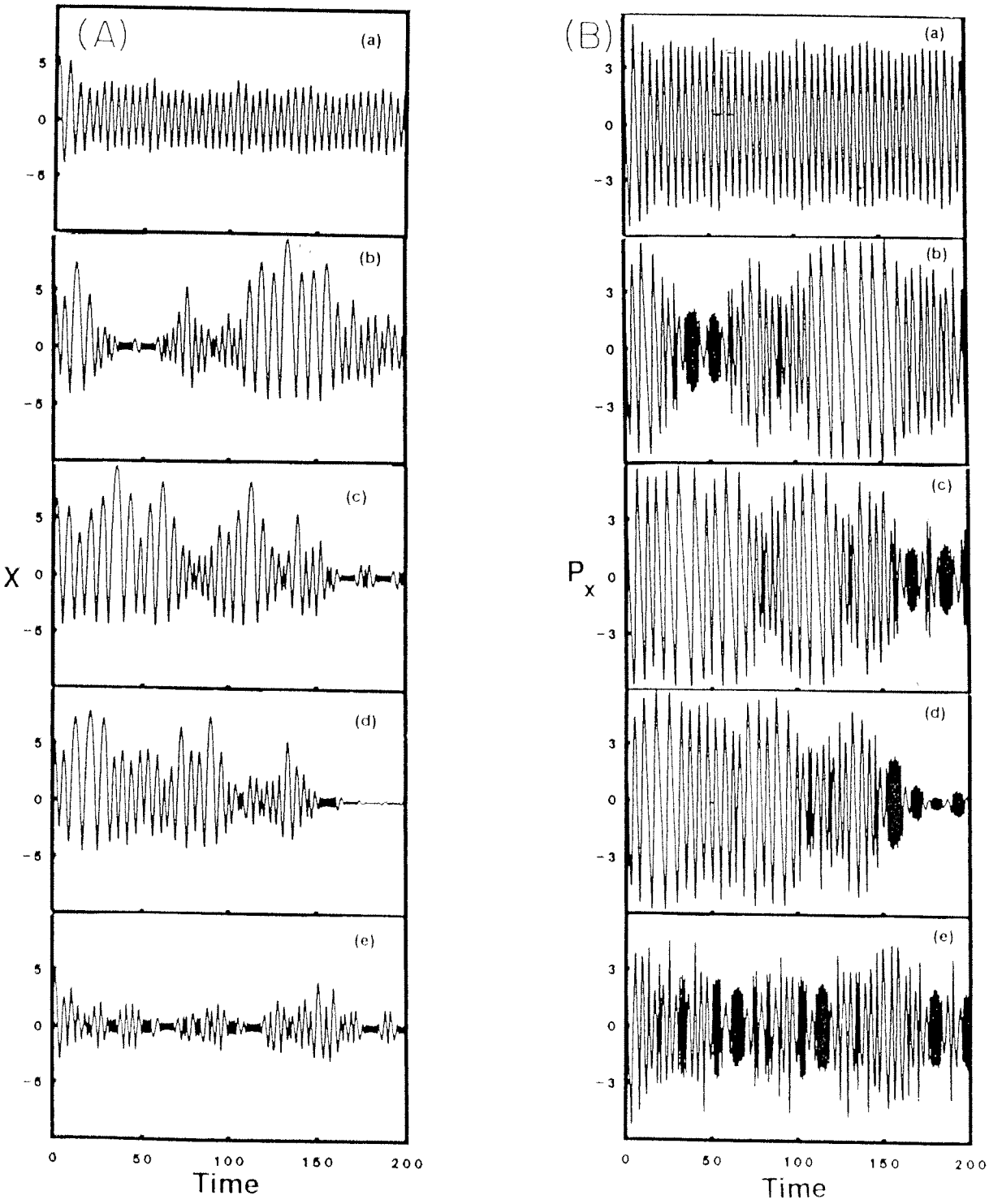

FIG. 5. (A) x for FC and MM trajectories. (a) Mixed mode, (b) trajectory no. 1, (c) trajectory no. 2, (d) trajectory no. 3, (e) trajectory no. 4. (B) p_x for FC and MM trajectories. (a) Mixed mode, (b) trajectory no. 1, (c) trajectory no. 2, (d) trajectory no. 3, (e) trajectory no. 4.

we do not know an accepted way of choosing clas-
ints that should correspond to a given wave pack-
e Wigner transformations [32] in general can be
r such phase space representations; however, they
rom the fact that they are not necessarily positive
domains of the phase space, which makes them
to employ as probability distributions. In many
Husimi transformations [33–36] are proposed to
the phase space, as they are positive definite in all
, but they are of only intuitive nature. However,
study, as we do not claim to exhaust the complete
l phase space, only a small number of trajectories
ılyzed, and there may be different procedures of
g these trajectories. We select four different FC trajectories whose energies are exactly the same as the MM case. These initial conditions are chosen such that

(a) and (b) the energy along the y coordinate and the coupling energy is the same in both the FC and MM cases; in this case, there are two y values with opposite signs (we choose only the positive momentum solutions).

(c) The classical y coordinate is the same as the expectation value over the wave packet.

(d) p_y is taken to be zero and y is obtained so that total energy is again the same.

Actual values of these coordinates and energy in modes and the coupling are given in Table I. These points sam-

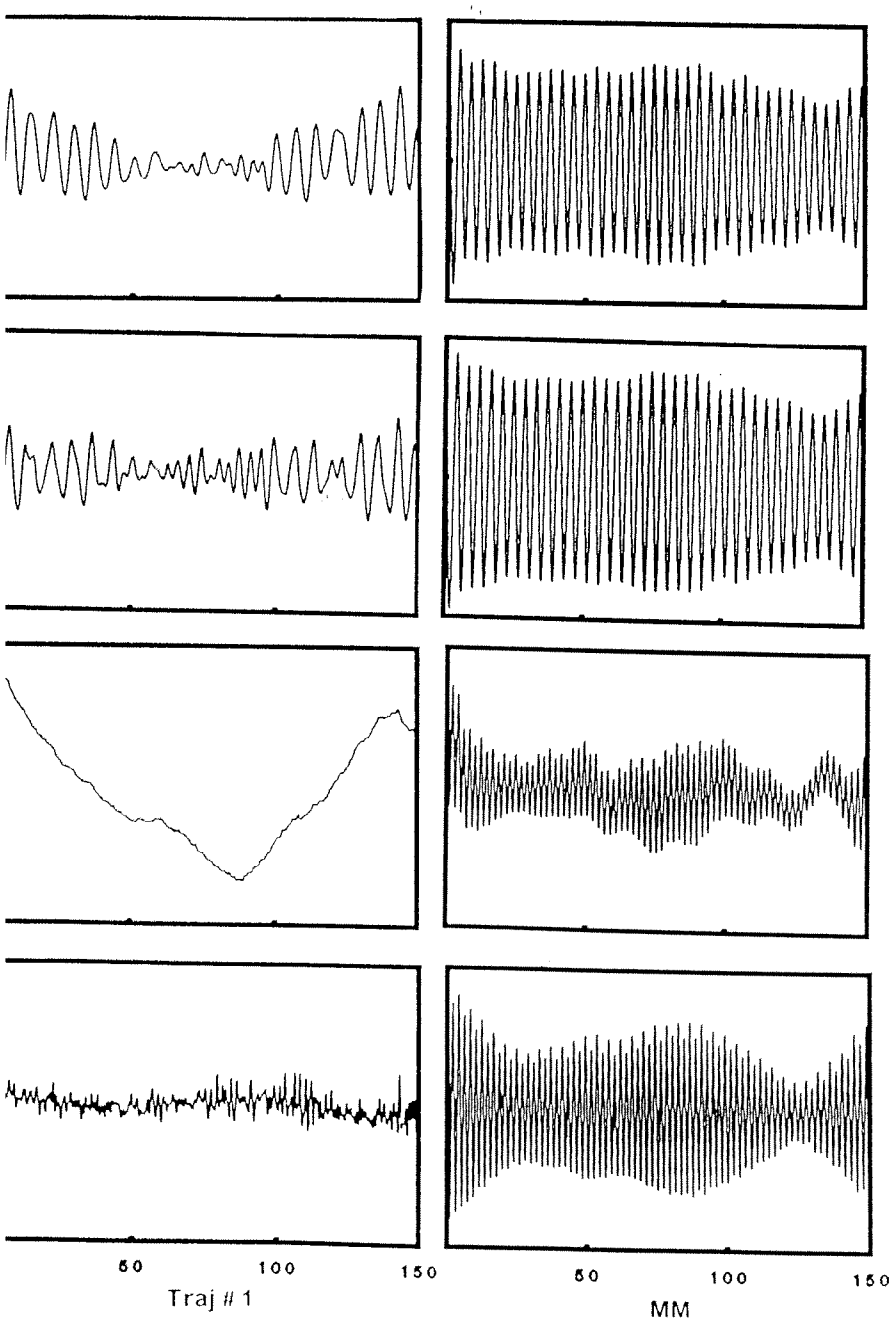

FIG. 6. Autocorrelation functions of x, P_x, E_x, and E_c for the classical trajectory no. 1 and MM.

ple the available phase space very sparsely, but as we see later they provide sufficient information on general trends. The maximum Lyapunov exponents for these initial conditions are 0.466, 0.449, 0.414, and 0.480 respectively. In Fig. 2, we present the Poincaré map, and in Fig. 3 various cross sections of the phase space for trajectory 1 are given. The other three trajectories give very similar trends, pointing out that indeed we are in the chaotic regime.

To compare two fundamentally different approaches poses some interesting problems, and one of them seems to be the partitioning of the coupling energy between two modes. That is, how does one define the energy of each mode? What are the contributions from the coupling energy? This separation is not unique and there is no standard method of determining the contributions to individual modes. Therefore, instead of computing energies of each mode in an arbitrary way, we proceed to define three energy terms E_x, E_y, and E_c, which are either classical observables, quantum expectation values, or a combination of them as in the case of E_c.

Since the x mode is always analyzed classically, it is more appropriate to compare properties of the FC and MM methodologies along the x coordinate. In Fig. 4, variations of E_x and E_c in time are given for the duration of 200 time units for the MM and four FC trajectories.

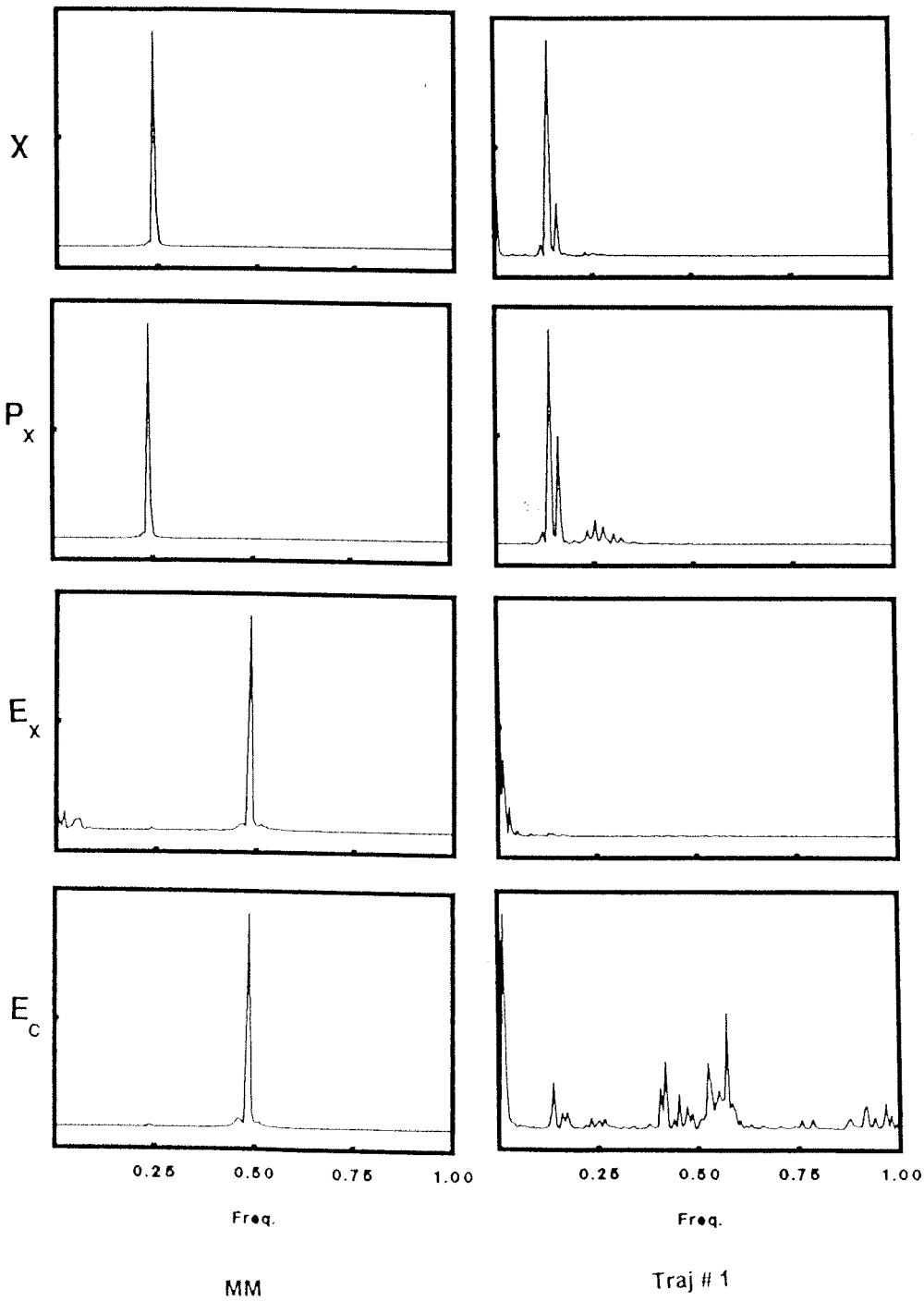

FIG. 7. Fourier transforms of autocorrelation functions of x, P_x, E_x, E_c.

'e observe two types of distinct behavior. In all FC trajectories, both amplitudes and frequencies of the oscillations display a large variety (longer time series for these assical calculations are also carried out, but here only ıe relatively short ones are presented in order to be able) display details). However, in the MM methodology, it clear that a great deal of periodicity appears in the corsponding time series. The variations of amplitudes are ubdued and the very periodic looking structures are notd. In fact, they all seem to be composed of superpositions of a few similar frequencies. This qualitative hange in the chaotic behavior is more pronounced for he coordinate and momentum along the x coordinate Fig. 5) where the motion in the classical phase space eems to be only a single frequency one. In classical nechanics, chaos is recognized by the sensitivity of the nitial conditions; that is, one asks the question of how fast the system forgets its past. One then can analyze the time autocorrelation functions, since they are thought to be memory functions.

$$C(\tau)=(1/N)\sum_{i=1}^{N} f(t)f(t+\tau)\ , \tag{22}$$

where f is the time-dependent function, τ is the correlation length, and N is the number of observations for the given τ. After normalization, $C(\tau)$ changes between -1 and 1, and any periodicity in it implies that the system still remembers its past history, which is a fingerprint of regular behavior. In Fig. 6, we display autocorrelation functions of x, p_x, E_x, and E_c for FC and MM cases. In classical calculations, autocorrelation functions go to zero quickly (sign of chaos) and then oscillate mildly around zero; however, those for the MM computations show strongly periodic structures. To determine the magnitudes of periodicity, we have obtained fast Fourier transformed (FFT) decompositions of autocorrelation functions (Fig. 7). As is expected, FFT transforms of FC trajectories show a variety of frequencies, whereas those of the MM trajectory display usually single sharp peaks. This final piece of evidence clearly points to a highly periodic and regular motion for MM dynamics.

We would like to summarize our findings in the following manner. In order to provide an opportunity to compare classical and quantum mechanical dynamics, we apply a mixed-mode formalism. Within this formalism, part of the system remains classical; therefore, exactly the same measures can be employed whether the system is fully classical or is under a partial quantization. For a reasonable comparison, we attempt to generate similar initial conditions for both approaches. Classical calculations under these conditions display highly chaotic behavior, as evidenced in the visual inspection of trajectories along a certain surface of sections and Lyapunov exponents. When we analyze several time-dependent properties, i.e., their autocorrelation functions and Fourier decompositions, we again note fingerprints of chaos. However, upon partial quantization, that is, by switching from the internal "classical" to "quantum" fields, radical changes in the qualitative behavior are observed. The time variations of classical energies and fields, radical changes in the qualitative behavior are observed. The time variations of classical energies and coordinates are no longer rich in frequencies, and they almost look "periodic." In fact, autocorrelation functions being highly periodic, we supply additional evidence to the disappearance of chaos, and FFT's fail to produce anything but single frequencies. It is reasonable to deduce from these facts that even a partial quantization smoothes out the chaotic details of a classical system. This is in accordance with our previous findings that a fully quantum description of a classically chaotic system displays a much more regular behavior than expected [28,29,37]. These results also provide additional evidence to the belief that bound systems of quantum systems cannot be chaotic [24,38].

ACKNOWLEDGMENTS

This project is supported by the TÜBiTAK, Grant No. TBAG-1218, as well as the NATO Grant No. GRG 900087. The author is grateful to J. Brickmann of Technische Hochschule Darmstadt for initiating this work.

[1] T. Uzer, Phys. Rep. **199**, 73 (1991).
[2] L. M. Raff and D. L. Thompson, *Theory of Chemical Reaction Dynamics*, edited by M. Baer (CRC, Boca Raton, FL, 1984), Vol. 3, p. 1.
[3] R. Kosloff, J. Phys. Chem. **92**, 2087 (1988).
[4] T. N. Truong, J. J. Tanner, P. Bala, J. A. McCammon, D. J. Kouri, B. Lesyng, and D. K. Hoffman, J. Chem. Phys. **96**, 2077 (1992).
[5] R. B. Gerber, V. Buch, and M. A. Ratner, J. Chem. Phys. **77**, 3022 (1982).
[6] R. Alimi, A. Garcia-Vela, and R. B. Gerber, J. Chem. Phys. **96**, 2034 (1992).
[7] A. J. Cruz and B. Jackson, J. Chem. Phys. **94**, 5715 (1991).
[8] E. Yurtsever and J. Brickmann, Ber. Bunsenges. Phys. Chem. **96**, 142 (1992).
[9] E. Yurtsever and T. Uzer, Ber. Bunsenges. Phys. Chem. **96**, 906 (1992).
[10] D. Farrelly and A. D. Smith, J. Phys. Chem. **90**, 1599 (1986).
[11] R. Alimi, R. B. Gerber, A. D. Hammerich, R. Kosloff, and M. A. Ratner, J. Chem. Phys. **93**, 6484 (1990).
[12] D. Farrelly and M. D. Emmel, Chem. Phys. Lett. **217**, 520 (1993).
[13] A. J. Lichtenberg and M. A. Lieberman, *Regular and Stochastic Motion* (Springer-Verlag, New York, 1993).
[14] M. C. Gutzwiller, *Chaos in Classical and Quantum Mechanics* (Springer-Verlag, Berlin, 1990).
[15] W. Dittrich and M. Reuter, *Classical and Quantum Dynamics* (Springer-Verlag, Berlin, 1992).
[16] F. Haake, *Quantum Signature of Chaos* (Springer-Verlag, Berlin, 1991).
[17] B. Eckhardt, Phys. Rep. **163**, 205 (1988).
[18] T. A. Brody, J. Flores, J. B. French, A. P. Mello, A. Pandey, and S. S. M. Wong, Rev. Mod. Phys. **53**, 385 (1982).
[19] T. Zimmermann, L. S. Cederbaum, H.-D. Meyer, and H. Köppel, J. Phys. Chem. **91**, 4447 (1987).

[20] N. Pomphrey, J. Phys. B **7**, 1909 (1974).
[21] D. W. Noid, M. L. Koszykowski, and R. A. Marcus, Ann. Rev. Phys. Chem. **32**, 267 (1981).
[22] J. Brickmann and R. L. Levine, Chem. Phys. Lett. **120**, 152 (1985).
[23] M. Shapiro, J. Ronkin, and P. Brumer, Ber. Bunsenges. Phys. Chem. **92**, 212 (1988).
[24] J. Ford and G.Mantica, Am. J. Phys. **60**, 1086 (1992).
[25] R. V. Jensen, Nature **355**, 311 (1992).
[26] W. H. Zurek, Phys. Today, **44** (10), 36 (1991).
[27] W. Slomczynski and K. Zyczkowski (unpublished).
[28] E. Yurtsever and J. Brickmann, Phys. Rev. A **41**, 6688 (1990).
[29] E. Yurtsever and J. Brickmann, Ber. Bunsenges. Phys. Chem. **94**, 804 (1990).
[30] J. Tobochnik and H. Gould, Comp. Phys. **3** (6), 86 (1989).
[31] A. Wolf, J. B. Swift, H. L. Swinney, and J. A. Vastano, Physica D **16**, 285 (1985).
[32] E. Wigner, Phys. Rev. **40**, 749 (1932).
[33] K. Husimi, Proc. Phys. Math. Soc. Jpn. **22**, 264 (1940).
[34] K. Zyczkowski, Phys. Rev. A **35**, 3546 (1987).
[35] K. Takahashi and N. Saito, Phys. Rev. Lett. **55**, 645 (1985).
[36] P. Al Jalil and E. Yurtsever, Tr. J. Phys. (to be published).
[37] E. Yurtsever, *Integrability and Chaotic Behavior*, edited by J. Seimenis (Kluwer, Dordrecht, in press).
[38] J. Manz, J. Chem. Phys. **91**, 2190 (1989).

BİBLİYOGRAFİK BİLGİ FORMU	
1- Proje No: TBAG-1218	2- Rapor Tarihi: Nisan 1995
3- Projenin Başlangıç ve Bitiş Tarihleri: 1.9.1993, 1.3.1995	
4- Projenin Adı: Klasik-Kuantum Moleküler Dinamik Yöntemi ile Titreşim Enerjisi Transferi	
5- Proje Yürütücüsü ve Yardımcı Araştırıcılar: Prof.Dr.Ersin YURTSEVER	
6- Projenin Yürütüldüğü Kuruluş ve Adresi: ODTÜ Kimya Bölümü	
7- Destekleyen Kuruluş(ların) Adı ve Adresi: TÜBİTAK	

8- Öz (Abstract):

Moleküliçi titreşim enerjisinin transferi, kontrollü reaksiyonları gerçekleştirmek isteyen bilim adamları için çok önemli bir konudur. Bu olayların mekanizmaları ve zaman ölçekleri, molekülde seçilmiş bağların oluşması veya kırılması için gerekli bilgiyi sağlarlar. Dinamik bir problemin kuantum mekaniksel analizi hesap zamanı açısından büyük güçlükler gösterir, buna karşılık klasik mekanik yöntemler ise sıfır noktası enerjisi veya tünelleme gibi olayları içermemeleri nedeni ile hatalı sonuçlara neden olabilirler. Bu çalışmada, her iki yaklaşımı birleştiren bir yöntem sunulmuş ve değişik uygulamaları tartışılmıştır. SCF yaklaşımı içerisinde problemin bir kısmı kuantum mekaniksel yollarla çözülmüş ve diğer kısımları ise klasik mekanik kanunlarınca yorumlanmıştır. Özellikle klasik kaosun, kısmi kuantumlaşma altında gösterdiği değişiklikler, kuantum dalgapaketine karşılık olabilecek faz uzayının tanımı ve bir boyutlu zincir üzerinde enerjinin transferi soruları çalışılmış, değişik çözüm yöntemleri geliştirilmiş ve bazı ipuçları elde edilmiştir.

Anahtar Kelimeler: Kuantum dinamiği, kaos, enerji transferi

9- Proje ile ilgili Yayın/Tebliğlerle ilgili Bilgiler: Yayınlar ektedir.	
10- Bilim Dalı: Fizikokimya Doçentlik B. Dalı Kodu: Uzmanlık Alanı Kodu:	ISIC Kodu:
11- Dağıtım (*) : ☐ Sınırlı	☒ Sınırsız
12- Raporun Gizlilik Durumu : ☐ Gizli	☒ Gizli Değil

(*) Projenizin Sonuç Raporunun ulaştırılmasını istediğiniz kurum ve kuruluşları ayrıca belirtiniz